

# Lecture 15

## *Explosive Nucleosynthesis and the r-Process*

As the shock wave passes through the star, matter is briefly heated to temperatures far above what it would have experienced had it burned in hydrostatic equilibrium. This material expands, then cools nearly adiabatically. The time scale for the cooling is approximately the *hydrodynamic time scale*, though a little shorter (because speeds are faster than free fall).

For (post-helium) burning in *hydrostatic equilibrium*, recall we had

$$\langle \epsilon_{\text{nuc}} \rangle \approx \langle \epsilon_{\text{v}} \rangle$$

*hydrostatic nucleosynthesis*  
*advanced stages of stellar evolution*

For *explosive nucleosynthesis* we have instead :

$$\tau_{\text{nuc}}(T_{\text{shock}}) \leq \tau_{\text{HD}}$$

$$\rho(t) = \rho_{\text{shock}} \exp(-t / \tau_{\text{HD}})$$

$$T(t) = T_{\text{shock}} \exp(-t / 3\tau_{\text{HD}})$$

$$\tau_{\text{HD}} = \frac{446 \text{ sec}}{\sqrt{\rho_{\text{shock}}}}$$

$$\rho \propto T^3$$

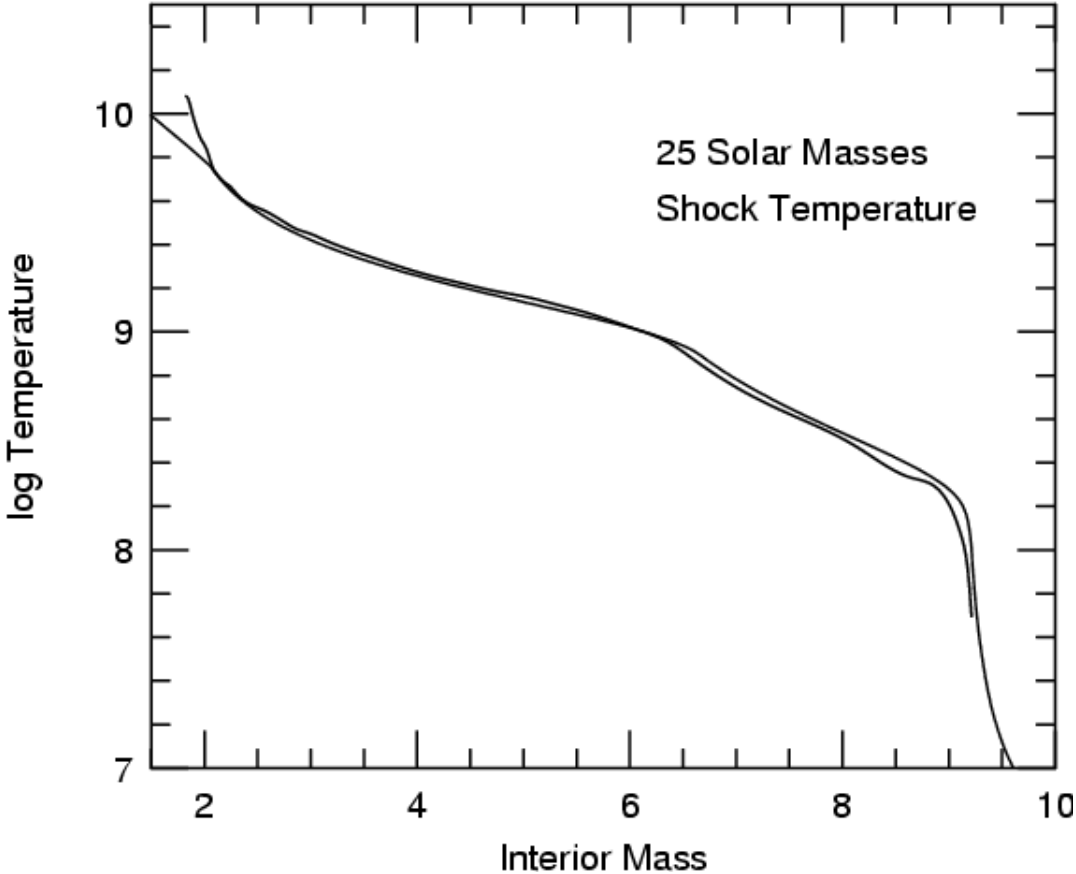
$$T_{\text{shock}} \approx 2.4 \times 10^9 R_9^{-3/4}$$

$$\rho_{\text{shock}} \approx 2 \rho_0$$

Except near the "mass cut", the shock temperature to which the explosive nucleosynthesis is most sensitive is given very well by

$$\frac{4}{3}\pi R^3 a T^4 \approx \text{Explosion energy}$$
$$\approx 10^{51} \text{ erg}$$

This is because of the near constancy of pressure behind the shock and the dominance of radiation



## Example:

Any carbon present inside of  $10^9$  cm will burn explosively since:

$$\text{At } T_9 = 2 \quad \lambda_{12,12} \approx 4.3 \times 10^{-4} \left(\frac{T_9}{2}\right)^{20}$$

$$\frac{dY_{12}}{dt} = -2 Y_{12}^2 \rho \lambda_{12,12} / 2$$

$$\tau_{12,12} = (\rho Y_{12} \lambda_{12,12})^{-1} = \frac{12}{\rho X_{12} \lambda_{12,12}} \quad X_{12} \approx 0.15$$

$$= 1.9 \left(\frac{2}{T_9}\right)^{20} = 45 / \sqrt{10^5} = 0.14 \text{ s} \quad \rho \sim 10^5$$

$$\Rightarrow \underline{\underline{T_9 = 2.3}}$$

0.1  $\tau_{\text{HD}}$

Where in the star does this occur?

$$10^{91} = \frac{4}{3} \pi R^3 \rho (2.3 \times 10^9)^4 \Rightarrow \underline{\underline{R = 1.0 \times 10^9 \text{ cm}}}$$

nb.  $T_p \propto R^{-3/4}$

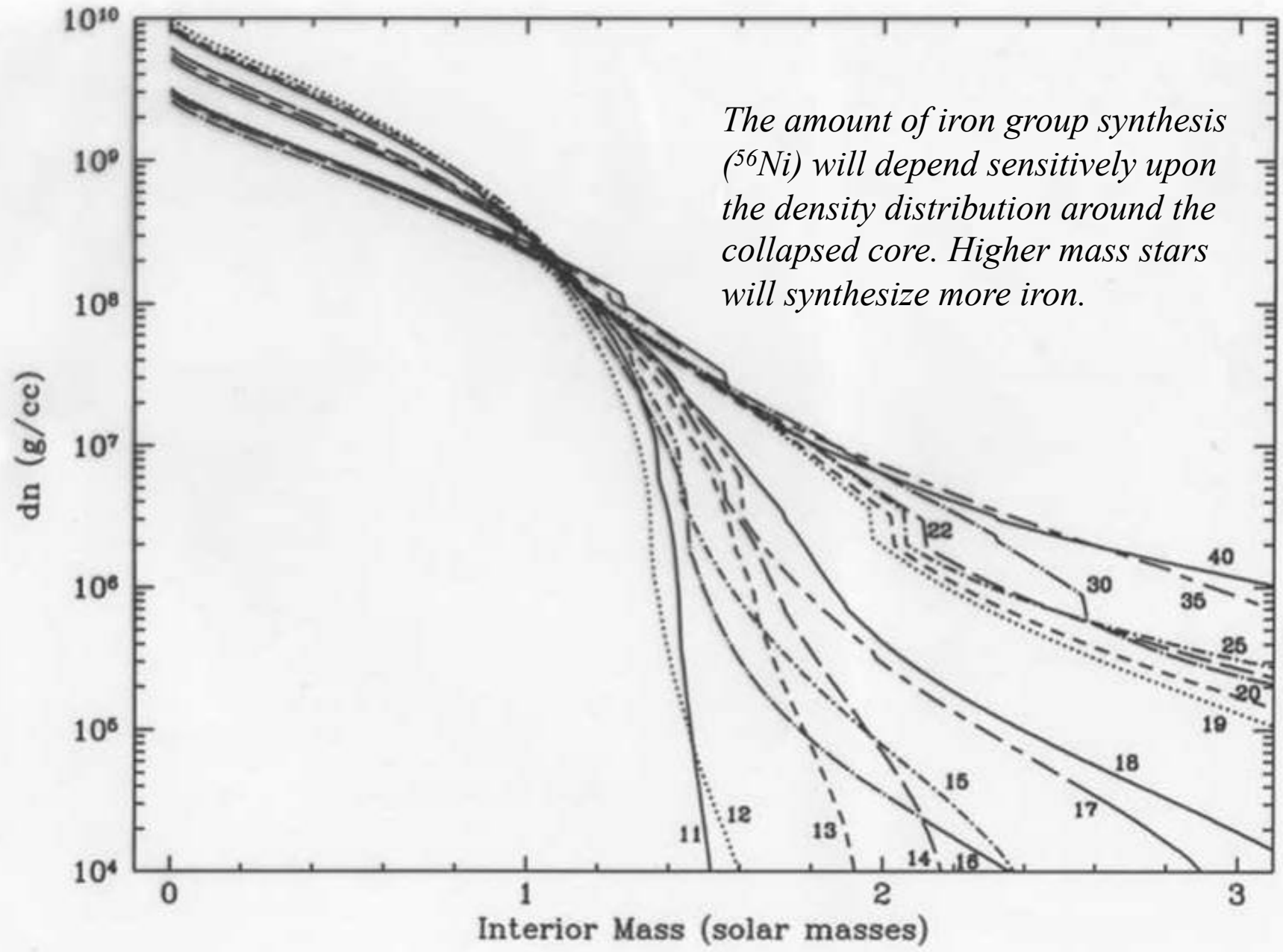
about 3.2  $M_{\odot}$  in  
the 25  $M_{\odot}$  presN star

Conditions for explosive burning in one 25 M<sub>⊙</sub> model (E<sub>0</sub> = 1.2 B):

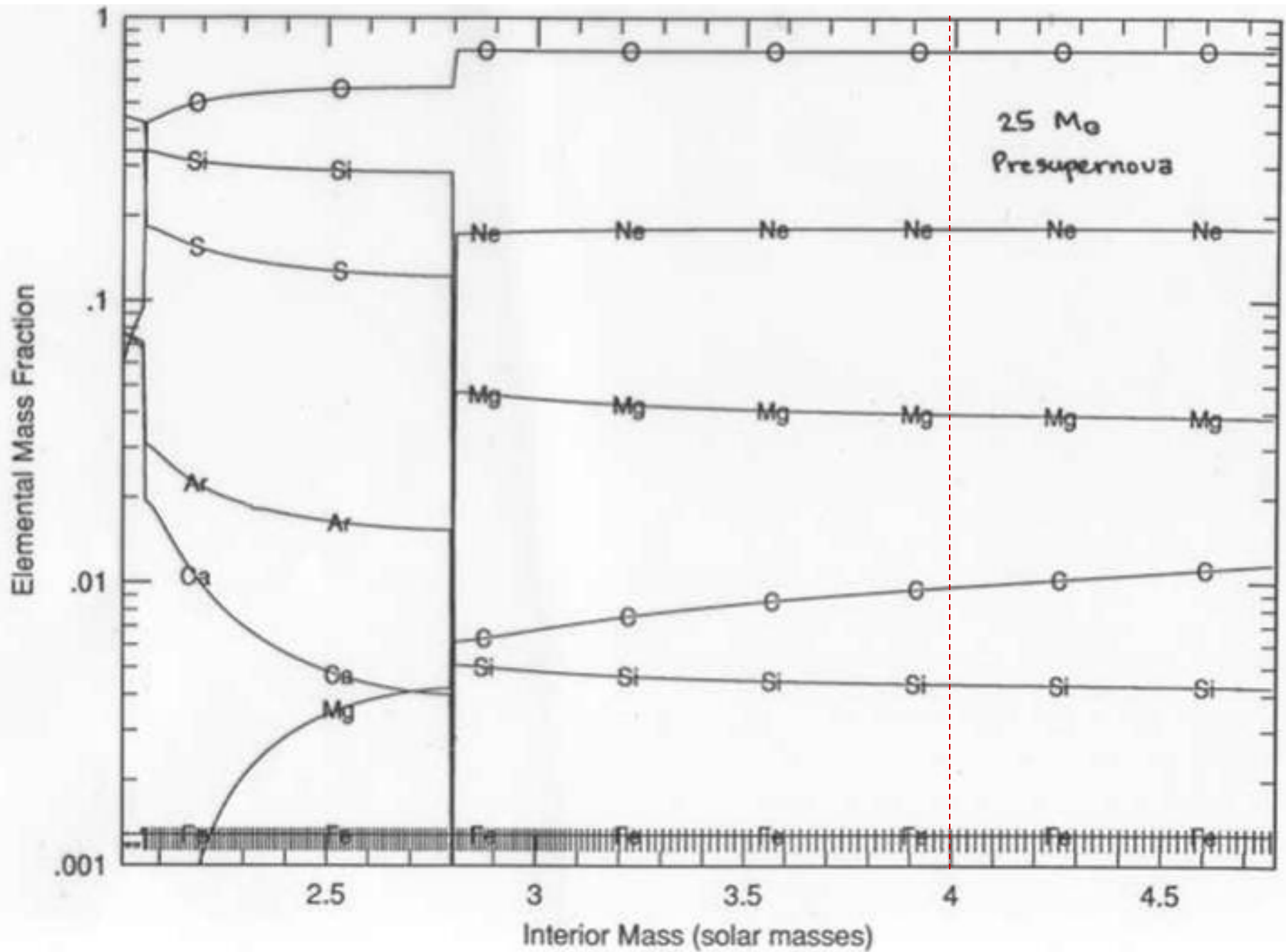
To use	$T_9 > 5$	$R_9 < 0.38$	<i>yes</i>
Silicon	4 – 5	0.38 – 0.51	<i>yes</i>
Oxygen	3 – 4	0.51 – 0.74	<i>yes</i>
Neon	2.5 – 3	0.74 – 1.0	<i>a little</i>
Carbon	2.0 – 2.5	1.0 – 1.3	<i>no</i>
Helium	>0.5	< 8	<i>no</i>
Hydrogen	>0.2	< 27	<i>no</i>

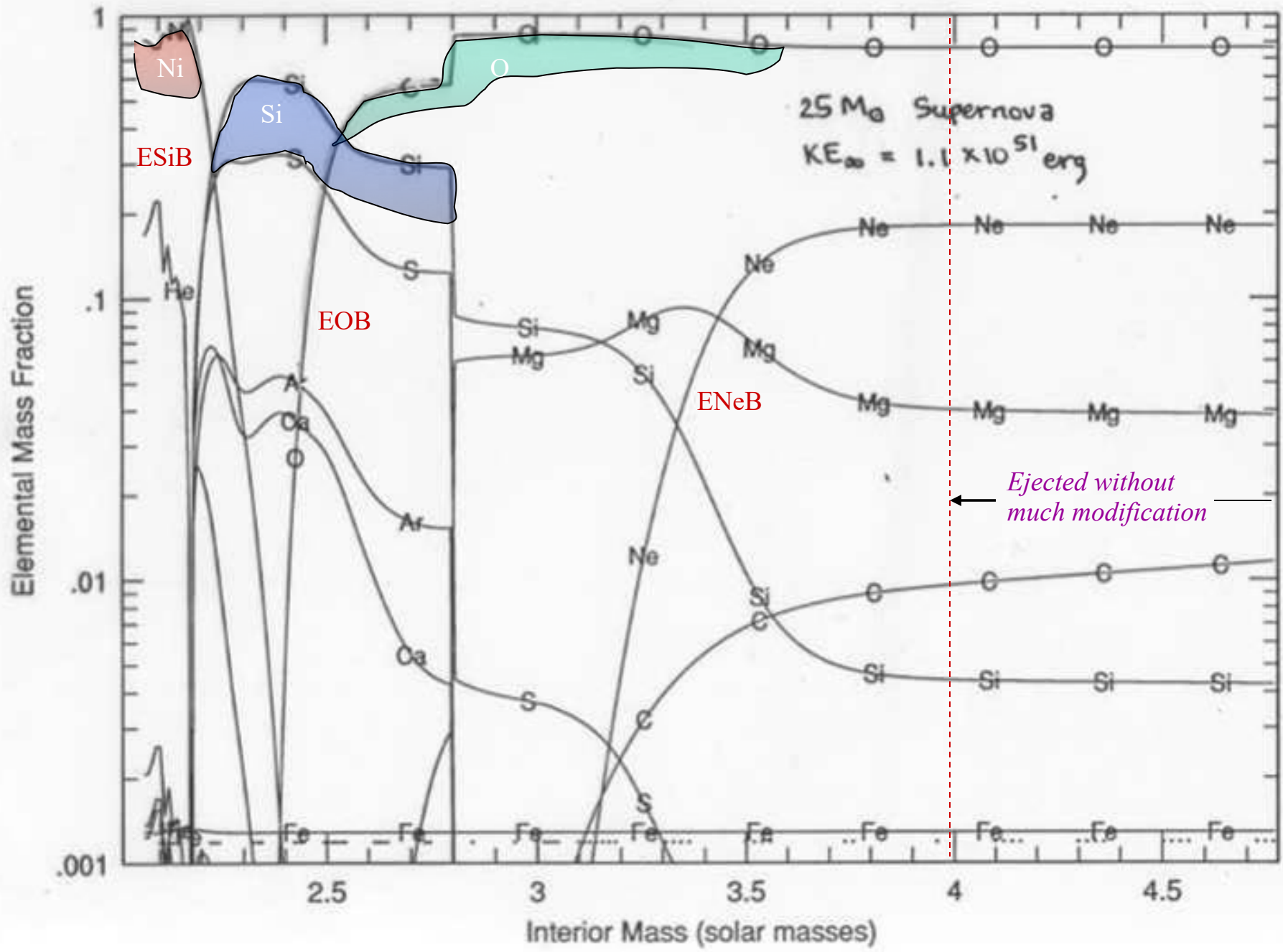
$$R_9 = \left( \frac{T_9}{2.4} \right)^{-4/3}$$

*Roughly speaking, everything that is ejected from inside 3800 km in the presupernova star will come out as iron-group elements.*



*The amount of iron group synthesis ( $^{56}\text{Ni}$ ) will depend sensitively upon the density distribution around the collapsed core. Higher mass stars will synthesize more iron.*





Produced pre-explosively and just ejected in the supernova:

- Helium
- Carbon, nitrogen, oxygen
- The s-process
- Most species lighter than silicon

Produced in the explosion:

- Iron and most of the iron group elements – Ti, V, Cr, Mn, Fe  
Co, Ni
- The r-process (?)
- The neutrino process – F, B

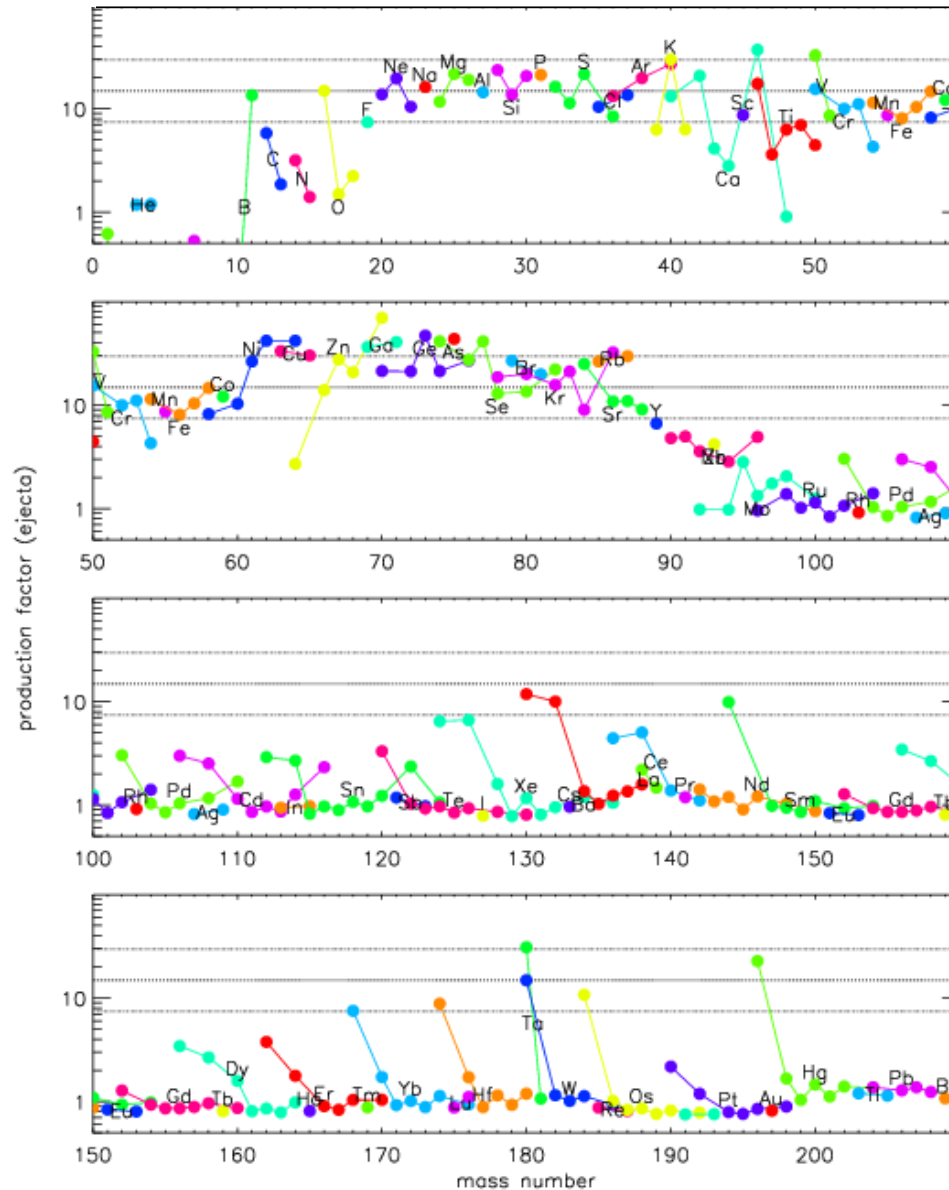
Produced both before and during the explosion:

- The intermediate mass elements – Si, S, Ar, Ca
- The p-process (in oxygen burning and explosive Ne burning)

# Explosive Nucleosynthesis

Fuel	Main Product	Secondary Products	Temp (10 <sup>9</sup> K)	Time (sec)
Innermost Ejecta	r- process	-	>10 low $Y_e$	about 1
Si, O	<sup>56</sup> Ni	Iron group	> 4	0.1
O	Si,S	Cl, Ar K, Ca	3 - 4	1
O, Ne	O, Mg Ne	Na, Al P	2 - 3	5
		p - process <sup>11</sup> B, <sup>19</sup> F	"	"

25 Solar Masses; Rauscher et al. (2002), parameterized explosion  
KE =  $1.2 \times 10^{51}$  erg at infinity (requires strong successful explosion)



The nucleosynthesis that results from explosive silicon burning is sensitive to the density (and time scale) of the explosion.

1) High density (or low entropy) NSE, and long time scale:

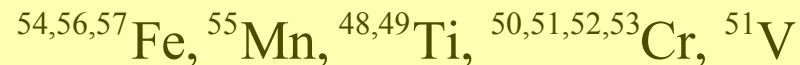
Either the material is never photodisintegrated even partially to  $\alpha$ -particles or else the  $\alpha$ -particles have time to reassemble into iron-group nuclei. The critical (slowest) reaction rate governing the reassembly is  $\alpha(2\alpha,\gamma)^{12}\text{C}$  which occurs at a rate proportional to  $\rho^2$ .

If as  $T \rightarrow 0$ ,  $X_n, X_p$ , and  $X_\alpha \rightarrow 0$  then one gets pretty much the unmodified "normal" results of nuclear statistical equilibrium calculated e.g., at  $T_9 = 3$  (fairly independent of  $\rho$ ).

Abundant nuclei at  $\eta = 0.002 - 0.004$

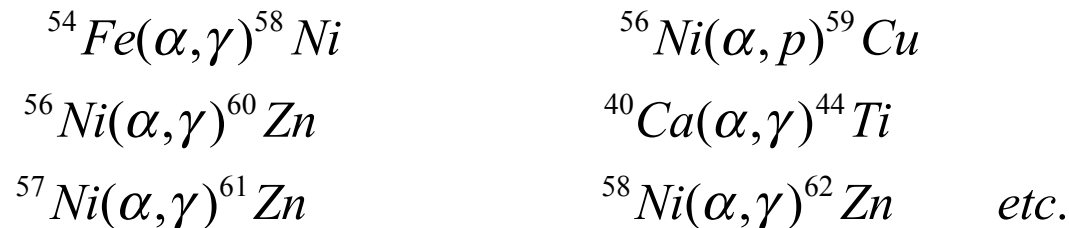


Products after all decays are complete:



2) Low density or rapid expansion → the “ $\alpha$ -rich” freeze out

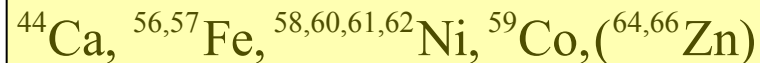
If all the  $\alpha$ 's from photodisintegration cannot reassemble on  $\tau_{\text{HD}}$ , then the composition will be modified at late times by  $\alpha$ -capture. The composition will "freeze out" with free  $\alpha$ -particles still present (and, in extreme cases, free n's or p's). The NSE composition at low T will be modified by reactions like



Abundant:



Produced :

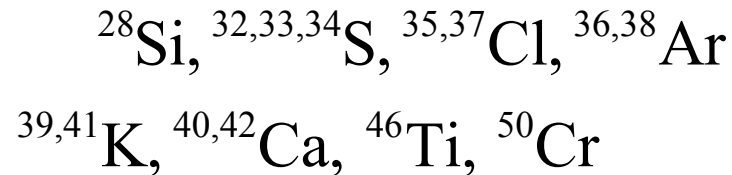


Both kinds of freeze-out occur in a typical explosion

### 3) Explosive oxygen burning ( $3 \leq T_9 \leq 4$ )

Makes pretty much the same products as ordinary oxygen burning ( $T_9 \approx 2$ ) at low  $\eta \approx 0.002$  ( $Z/Z_\odot$ )

Principal Products:



### 4) Explosive neon and carbon burning ( $2 \leq T_9 \leq 3$ )

Same products as stable hydrostatic burning

More  ${}^{26}\text{Al}$ , **the p-process or  $\gamma$ -process.**

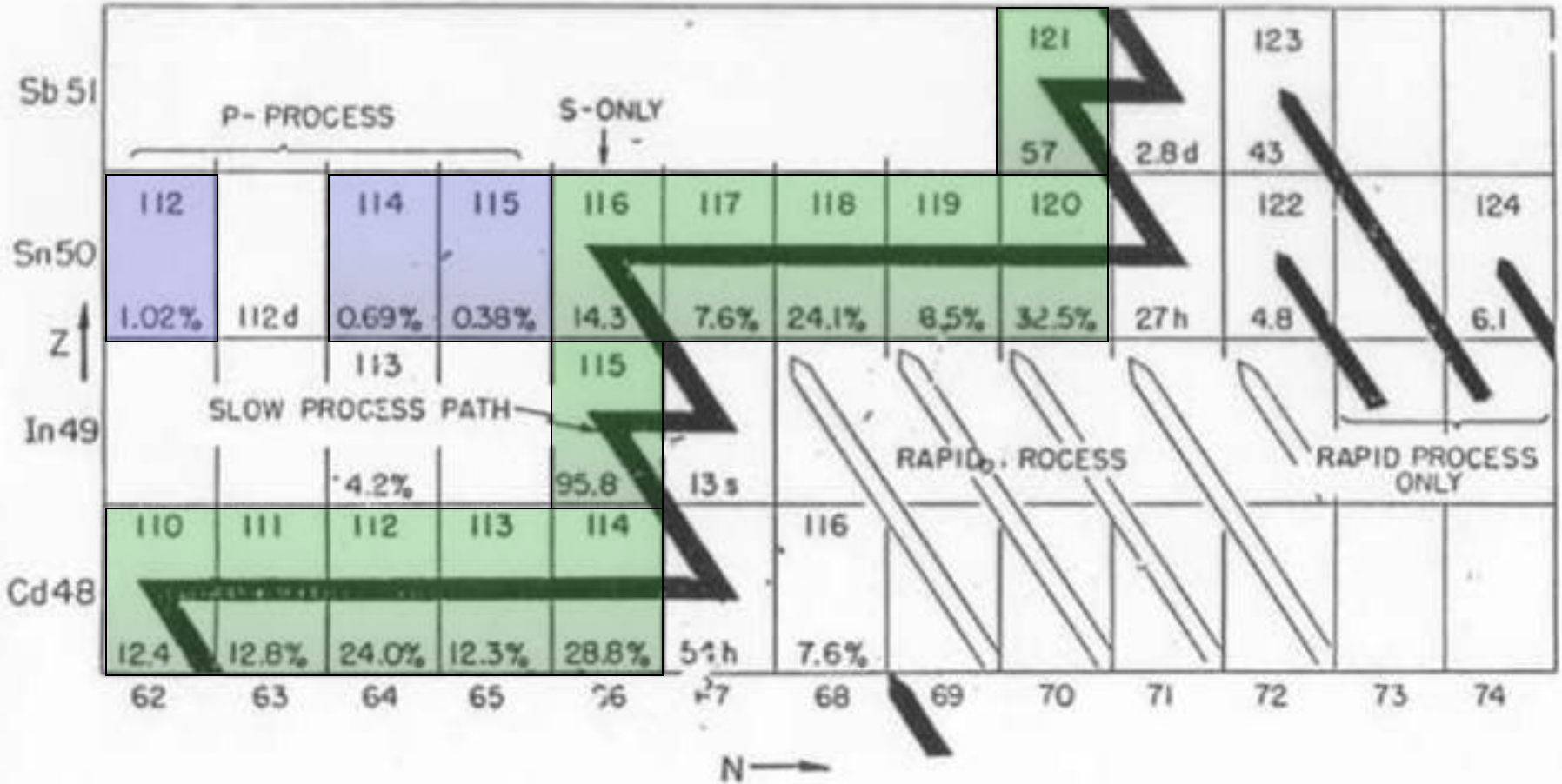
### 5) Explosive H and explosive He burning.

The former occurs in novae; the latter in some varieties of Type Ia supernovae. Discuss later.

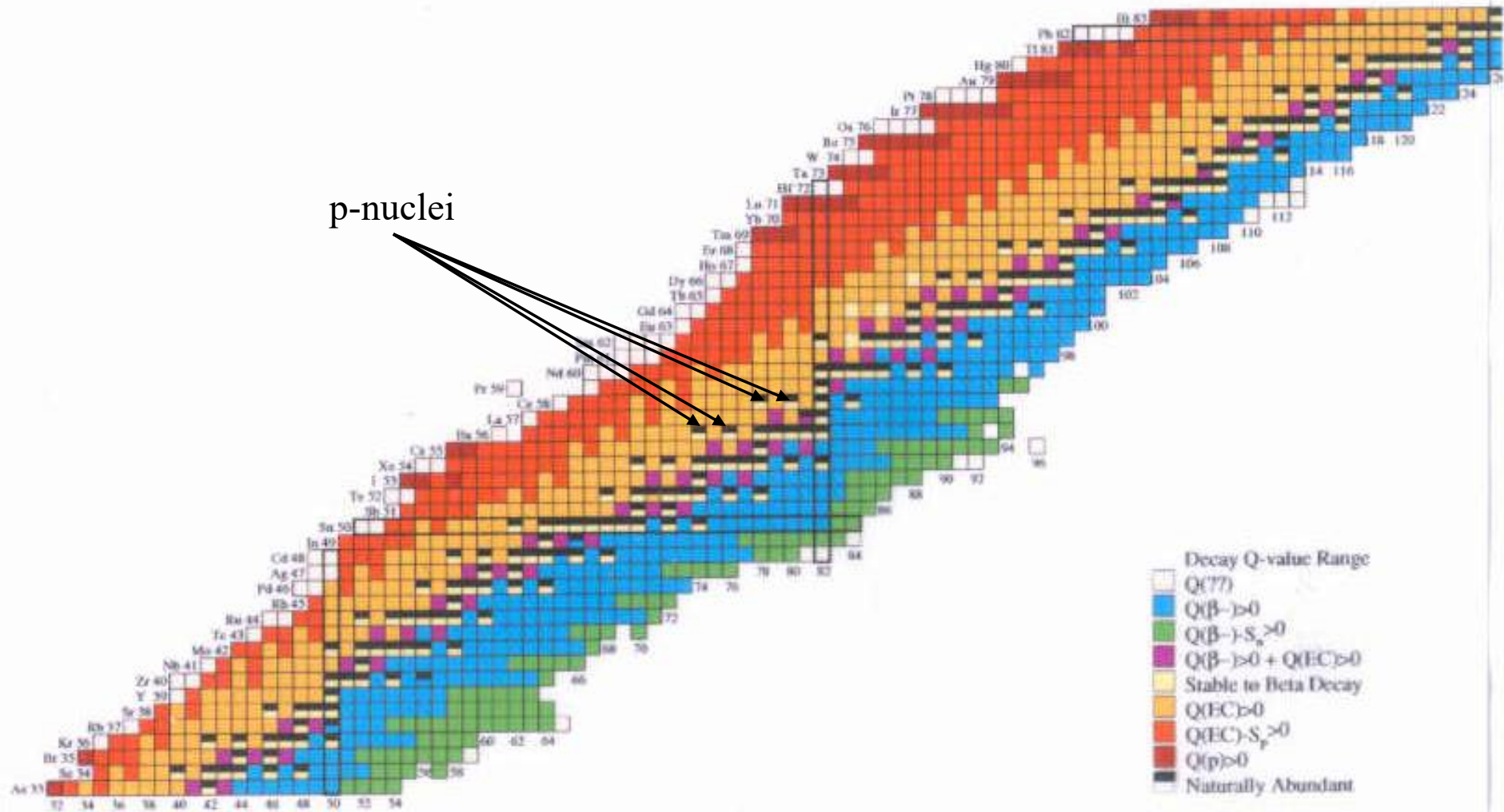
# *The “p - ” or $\gamma$ - Process*

*At temperatures  $\sim 2 \times 10^9$  K before the explosion (oxygen burning) or between 2 and  $3.2 \times 10^9$  K during the explosion (explosive neon and oxygen burning) partial photodisintegration of pre-existing s-process seed makes the proton-rich elements above the iron group.*

# The $p$ -Process (aka the $\gamma$ -process)



# *p*-Process Nuclei



p-nuclei



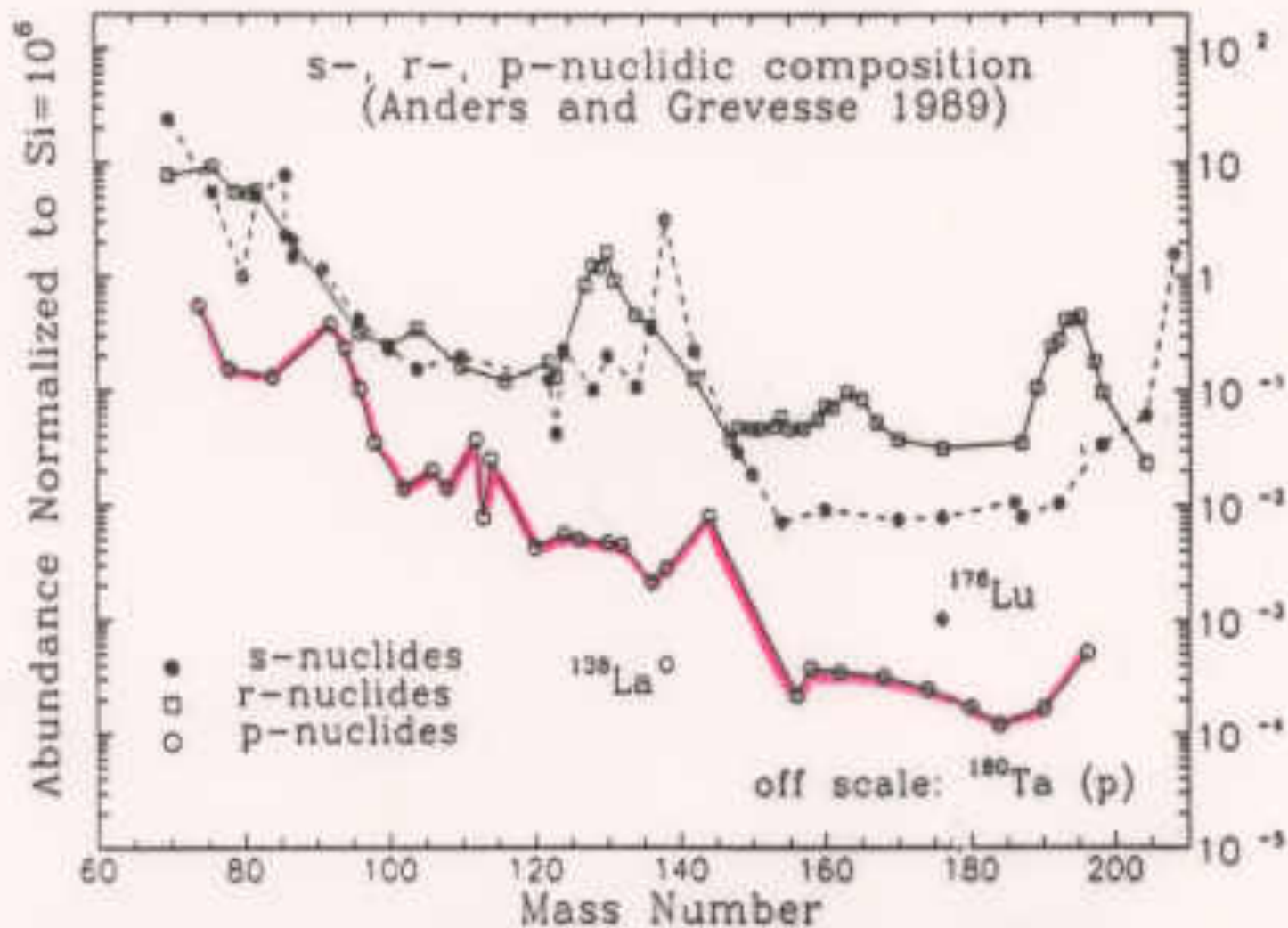
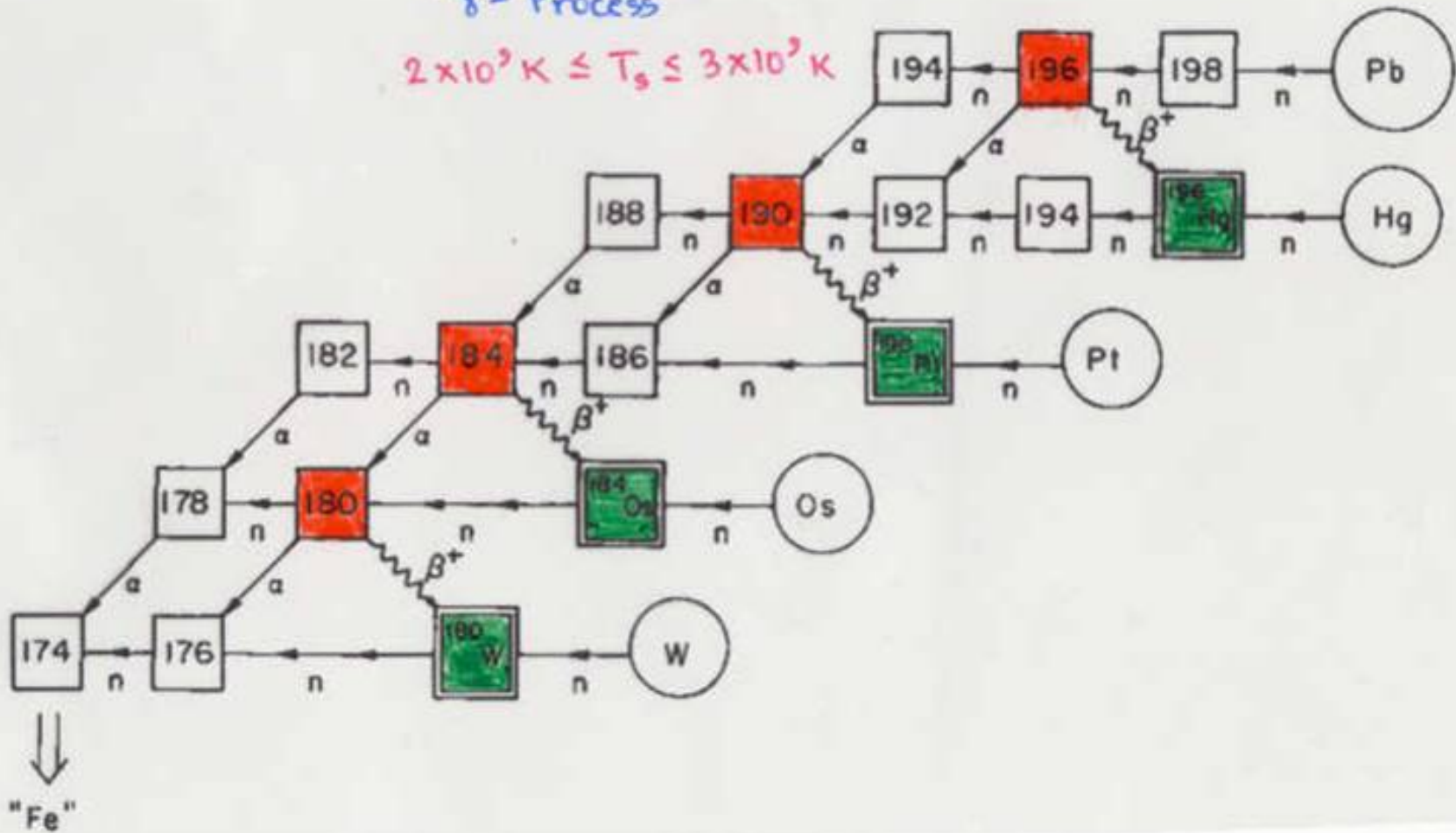


Fig. 1. Abundances of p, r, and s-nuclides in the SAD (Anders and Grevesse 1989). Note that <sup>180</sup>Ta has the very low abundance of  $2.5 \times 10^{-6}$ . (From Amoult 1991)

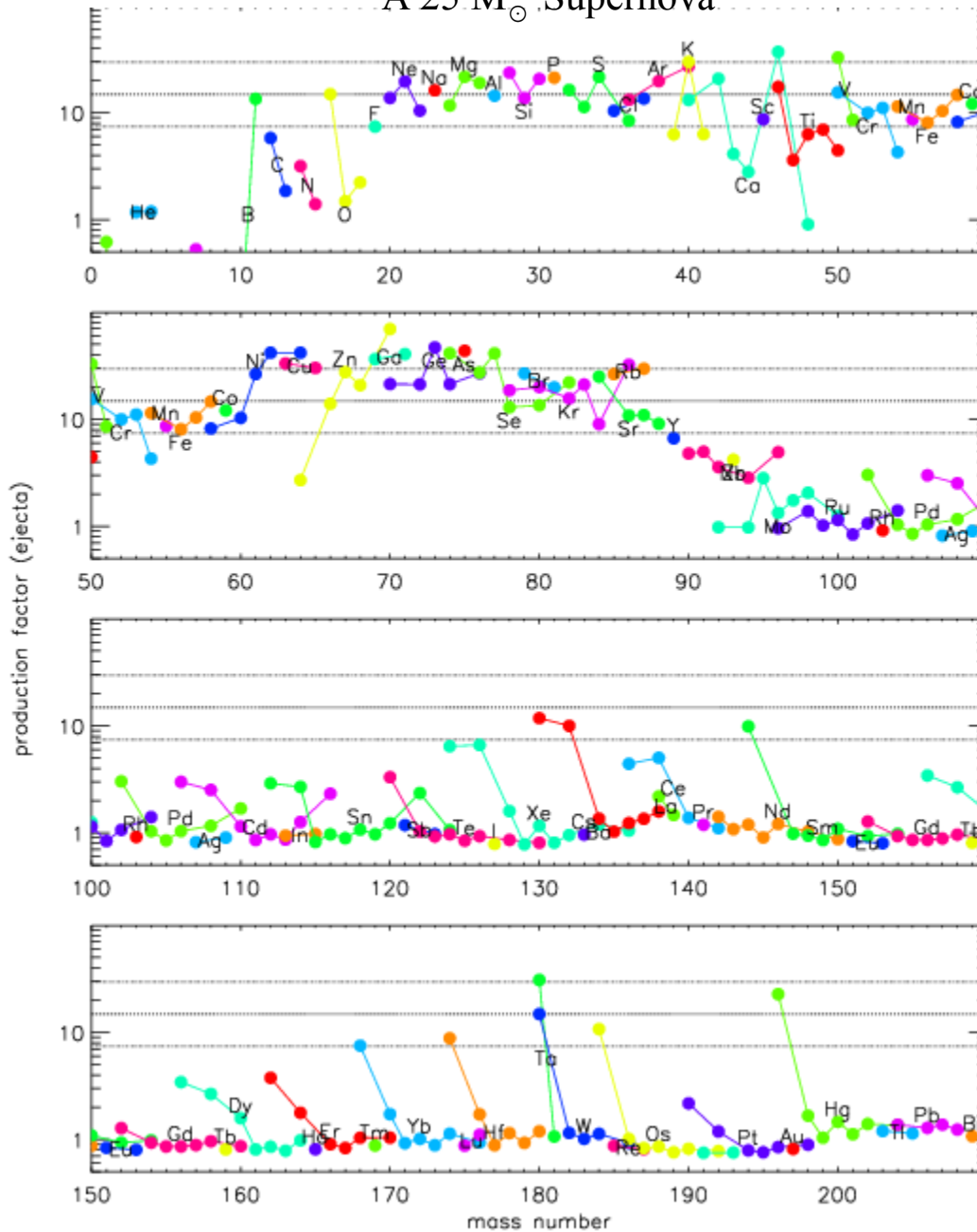
# WOOSLEY AND HOWARD

" $\gamma$ -Process"

$$2 \times 10^9 \text{ K} \leq T_s \leq 3 \times 10^9 \text{ K}$$



# A 25 M<sub>⊙</sub> Supernova



Problems below  
A ~ 130.

## Summary: $\gamma$ –Process

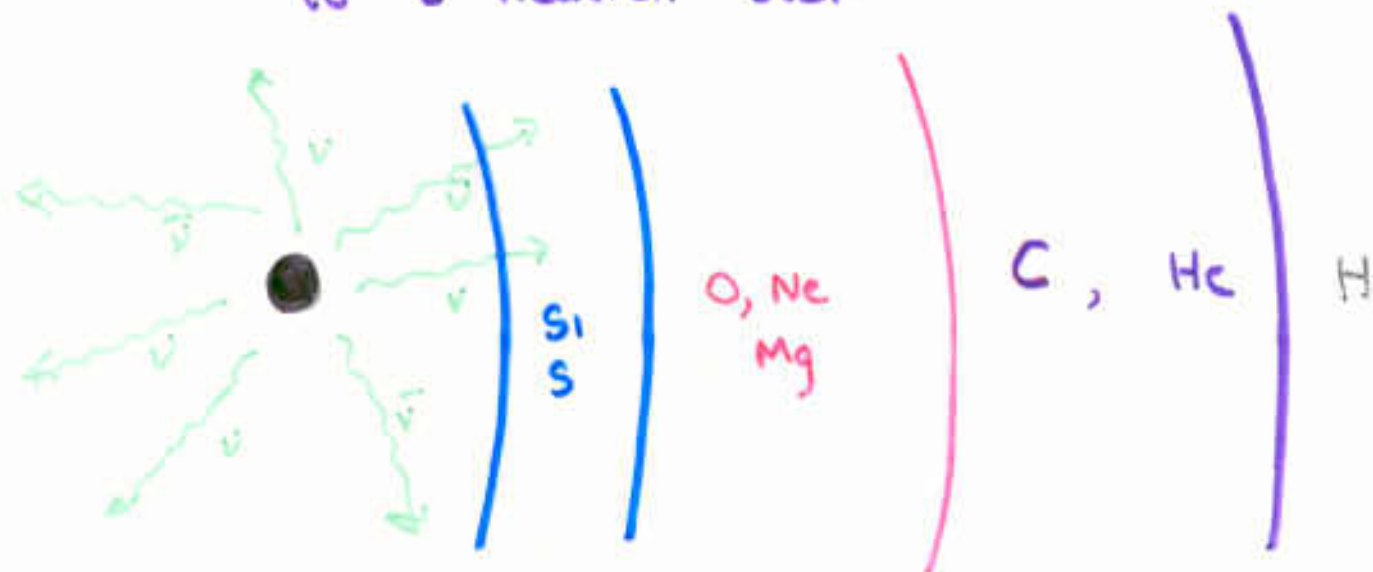
- Makes nuclei traditionally attributed to the “p-process” by photodisintegration of pre-existing s-process nuclei. The abundance of these seeds is enhanced – at least for  $A < 90$  – by the s-process that went on in He and C burning.
- Partially produced in oxygen shell burning before the collapse of the iron core, but mostly made explosively in the carbon, neon, and oxygen-rich shells that experience shock temperatures between 2 and 3.2 billion K.
- Production factor  $\sim 100$  in about 1 solar mass of ejecta. Enough to make solar abundances
- A secondary (or tertiary) process. Yield is proportional to abundance of s-process in the star.
- There remain problems in producing sufficient quantities of p-nuclei with atomic masses between about 90 and 120, especially  $^{92}\text{Mo}$ .

# *The Neutrino Process*

## *( $\nu$ -process)*

*The neutrino flux from neutron star formation in the center can induce nuclear transmutation in the overlying layers of ejecta. The reactions chiefly involve  $\mu$  and  $\tau$ -neutrinos and neutral current interactions. Notable products are  $^{11}\text{B}$ ,  $^{19}\text{F}$ ,  $^{138}\text{La}$ ,  $^{180}\text{Ta}$ , and some  $^7\text{Li}$  and  $^{26}\text{Al}$ .*

Now the iron core collapses  
to a neutron star



$$L_{\nu} \approx 10^{53} \text{ erg/s}$$

i.e.  $0.05 M_{\odot} c^2 / \text{s}$

$$\underbrace{\nu_e, \bar{\nu}_e}_{\sim 4 \text{ MeV}}, \underbrace{\nu_{\mu}, \bar{\nu}_{\mu}, \nu_{\tau}, \bar{\nu}_{\tau}}_{\sim 6-8 \text{ MeV}}$$

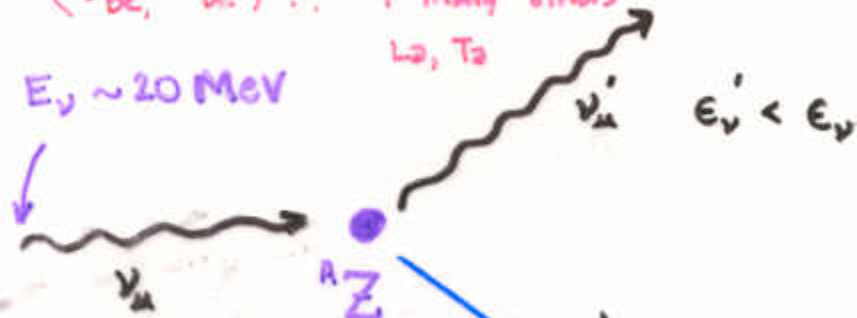
for  $\sim 3$  seconds

Woodsley, Hartmann, Hoffman, + Haxton  
(1990)

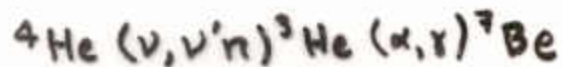
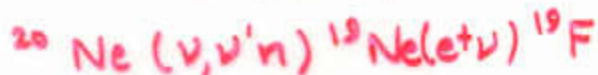
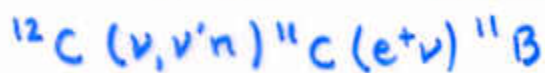
Responsible for  
(some)  ${}^7\text{Li}$ ,  ${}^{11}\text{B}$ ,  ${}^{19}\text{F}$   
( ${}^9\text{Be}$ ,  ${}^{10}\text{Be}$ ) ??

contributions to  
+ many others  
 $L_2, T_2$

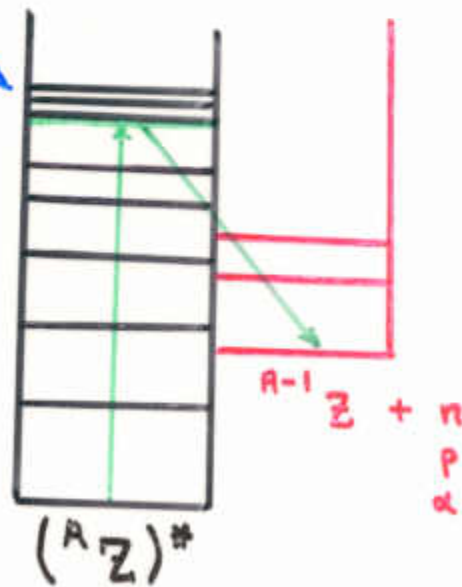
$E_\nu \sim 20 \text{ MeV}$



Examples:



+ secondary reactions



*Production factor relative to solar normalized to  $^{16}\text{O}$  production as a function of  $\mu$  and  $\tau$  neutrino temperature (neutral current) and using 4 MeV for the electron (anti-)neutrinos (for charged current only). 6 MeV is now considered a more likely value for  $T_{\mu\tau}$*

Product	$15 M_{\odot}$				$25 M_{\odot}$			
	6 MeV		8 MeV		6 MeV		8 MeV	
	WW95	This work	WW95	This work	WW95	This work	WW95	This work
$^{11}\text{B}$	1.65	1.88	3.26	3.99	0.95	1.18	1.36	1.85
$^{19}\text{F}$	0.83	0.60	1.28	0.80	0.56	0.32	1.03	0.53
$^{15}\text{N}$	0.46	0.49	0.54	0.58	0.09	0.12	0.15	0.19
$^{138}\text{La}$		0.97		1.10		0.90		1.03
$^{180}\text{Ta}$		2.75		3.07		4.24		5.25

# *Integrated Ejecta*

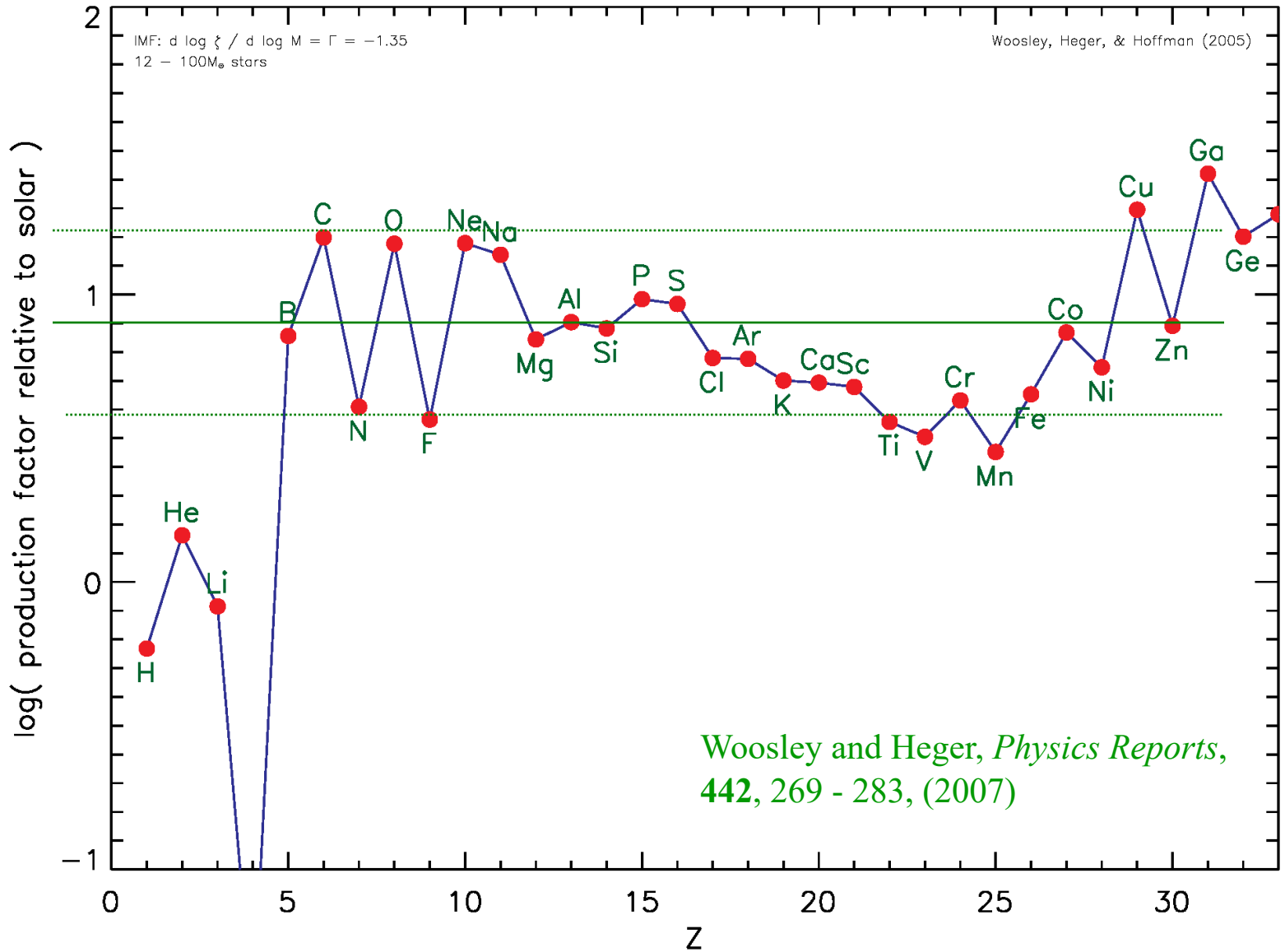
*Averaged yields of many supernovae  
integrated either over an IMF or a model  
for galactic chemical evolution.*

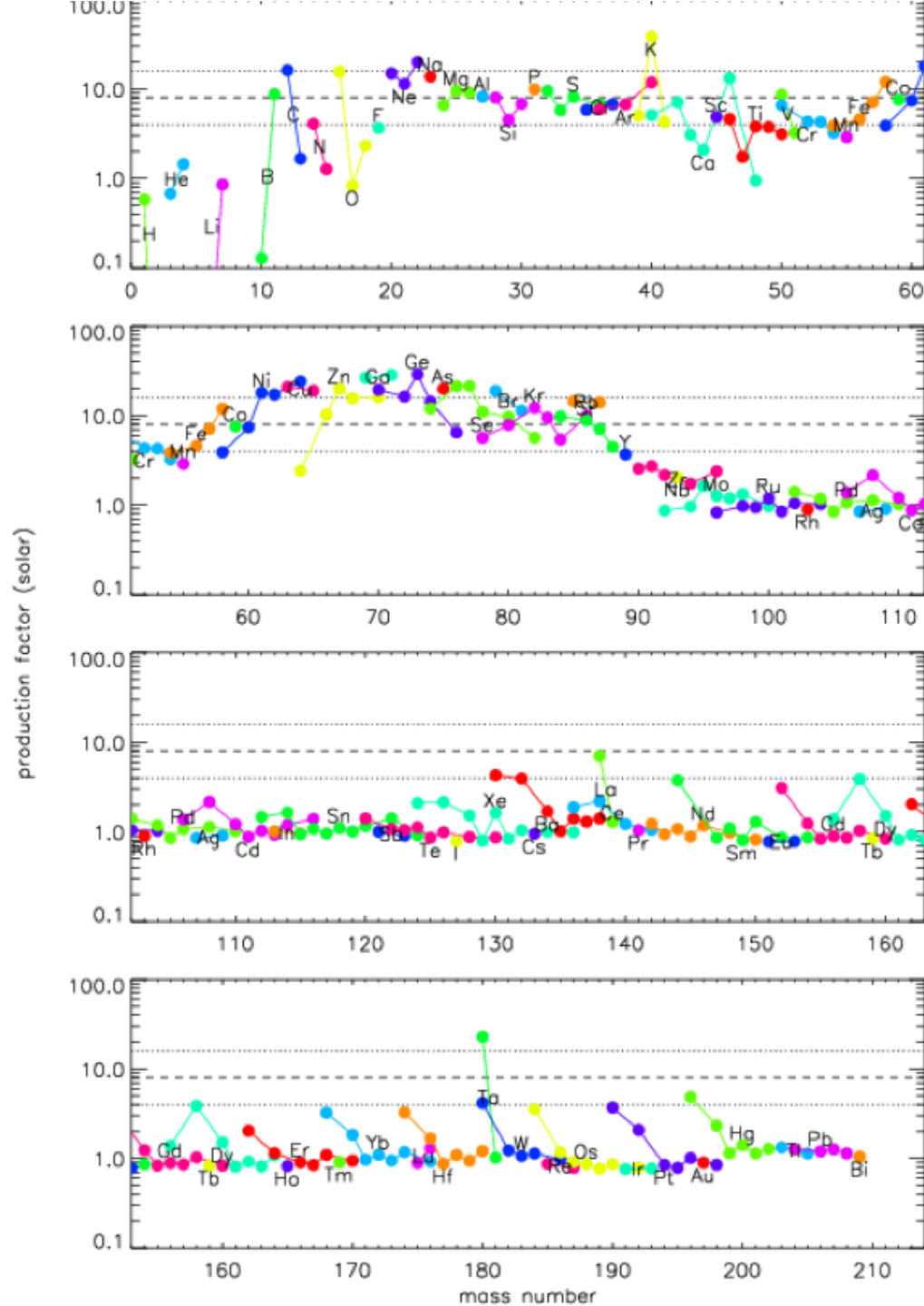
# Survey - Solar metallicity:

(Woosley and Heger 2007)

- *Composition – Lodders (2003); Asplund, Grevesse, & Sauval (2004)*
- *32 stars of mass 12, 13, 14, 15, 16, 17, 18, 19, 20, 21, 22, 23, 24, 25, 26, 27, 28, 29, 30, 31, 32, 33, 35, 40, 45, 50, 55, 60, 70, 80, 100, 120 solar masses.*
- *Evolved from main sequence through explosion with two choices of mass cut ( $S/N_A kT = 4$  and Fe-core) and two explosion energies (1.2 B, 2.4 B) – 128 supernova models*
- *Averaged over Salpeter IMF*

# Production Factor 12 – 100 solar masses 1.2 foe explosions





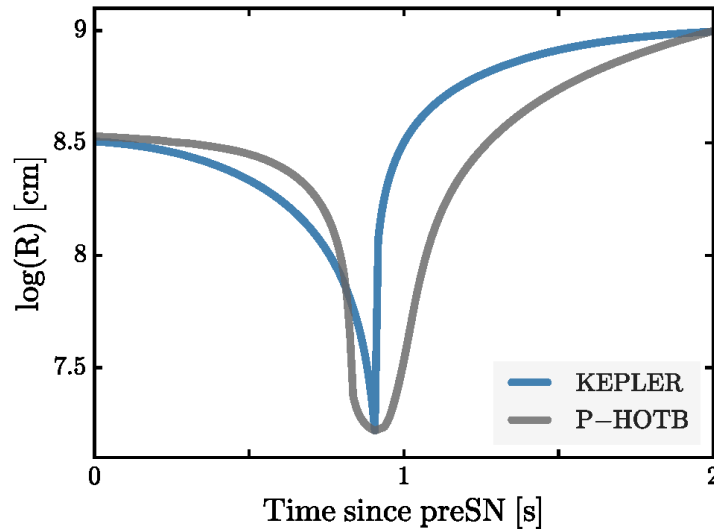
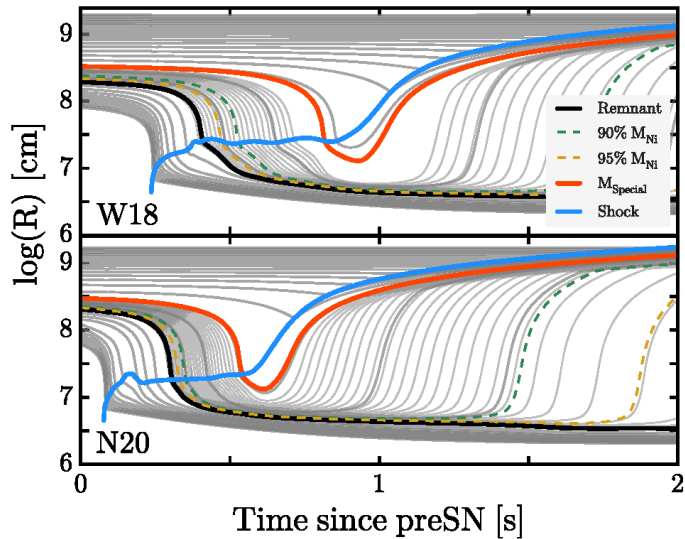
*Isotopic yields for 31 stars averaged over a Salpeter IMF,  $\Gamma = -1.35$*

*Intermediate mass elements ( $23 < A < 60$ ) and s-process ( $A = 60 - 90$ ) well produced.*

*Carbon and Oxygen over-produced.*

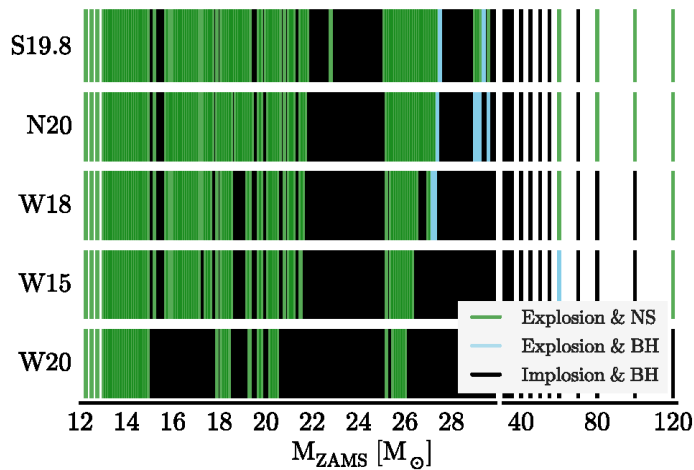
*p-process deficient by a factor of  $\sim 4$  for  $A > 130$  and absent for  $A < 130$*

# Sukhbold et al (2016) – 300 supernova models – 2000 nuclei

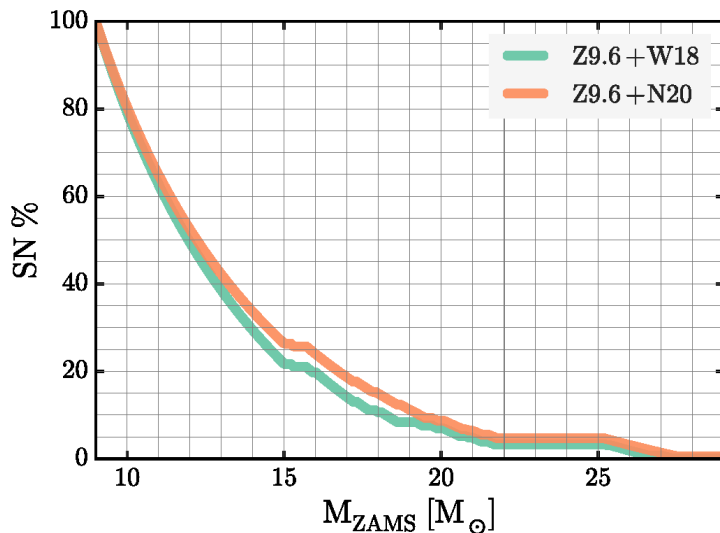


Ertl and Janka (P-HOTB)

Mapped into KEPLER



Successful explosions  
in green

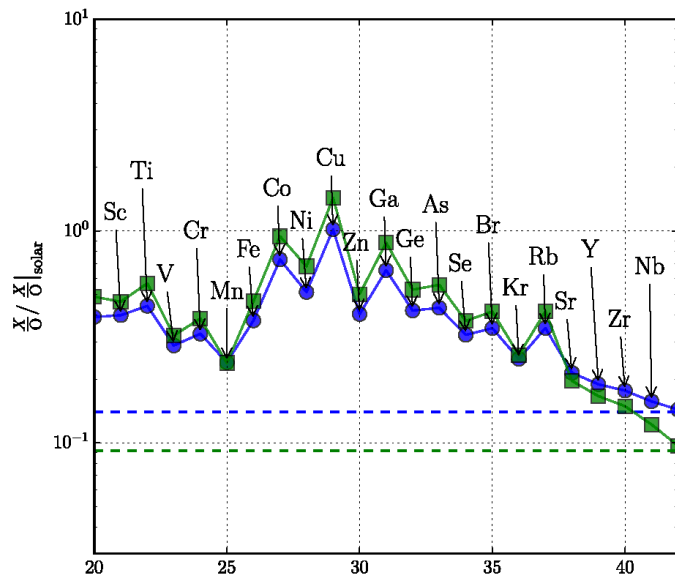
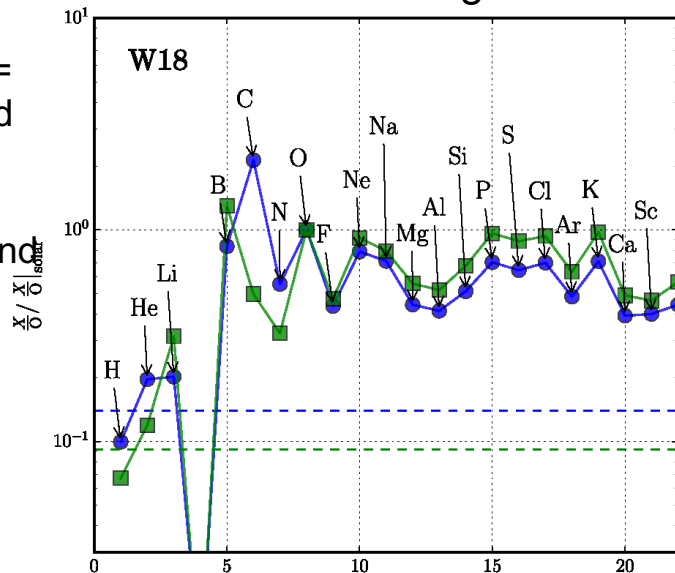


Fraction of supernovae

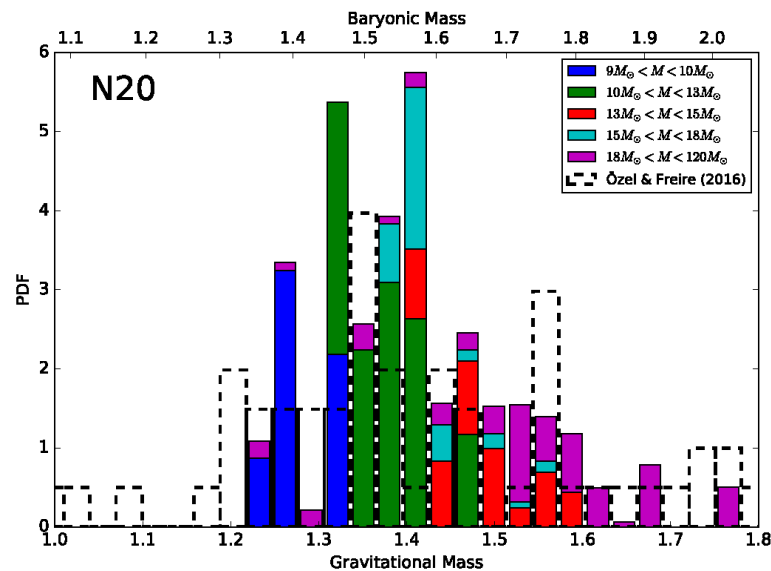
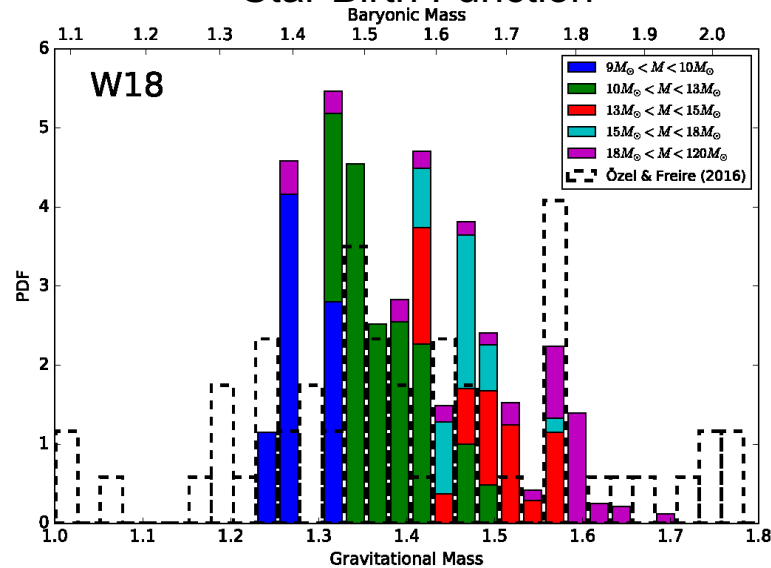
## IMF Averages for 2 Central Engines

green =  
no wind

blue =  
with wind



## IMF Weighted Neutron Star Birth Function



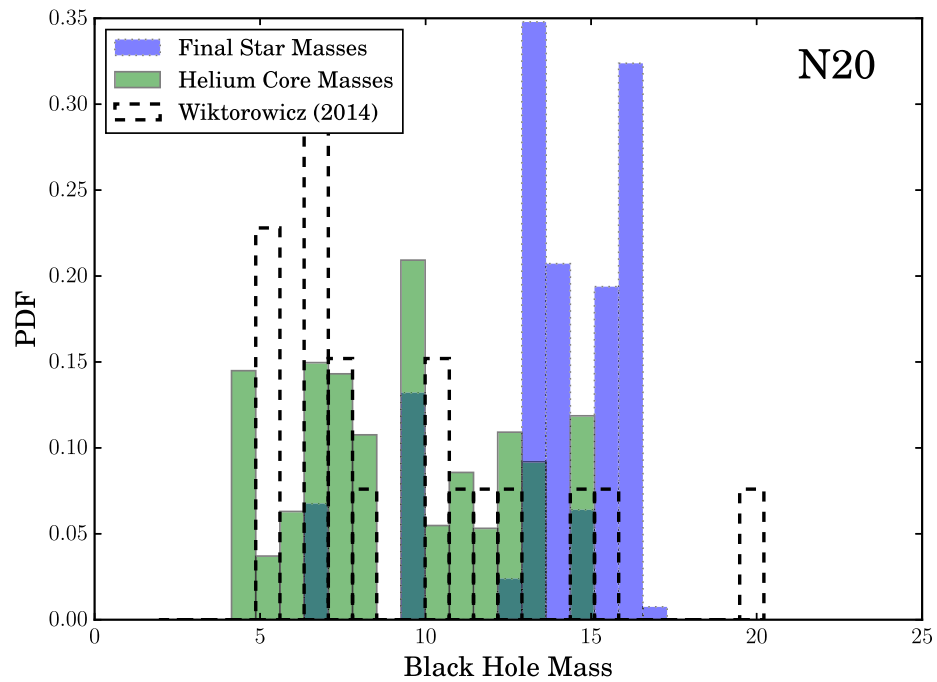
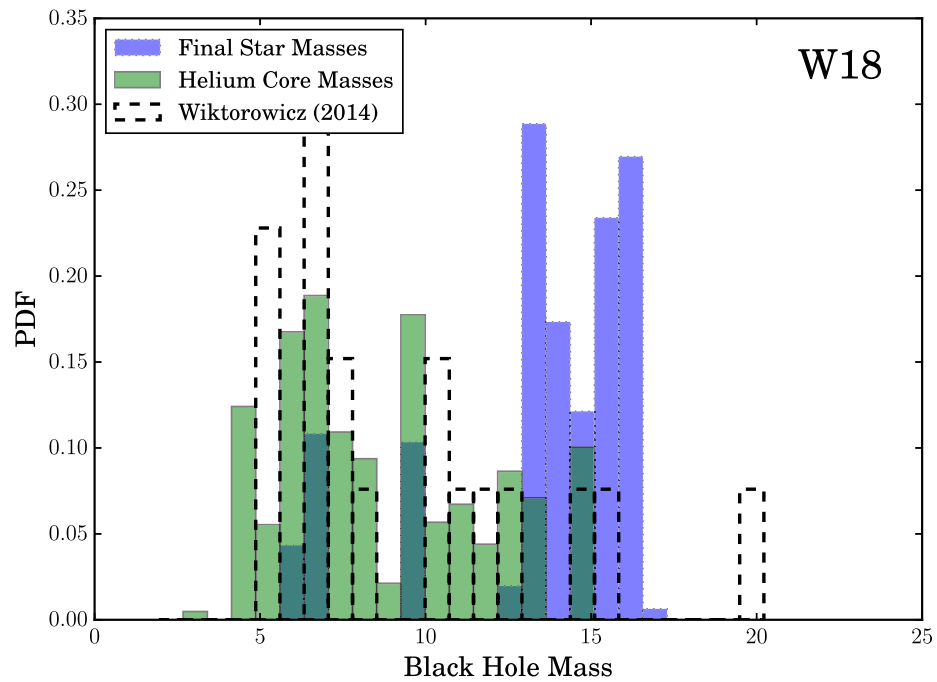
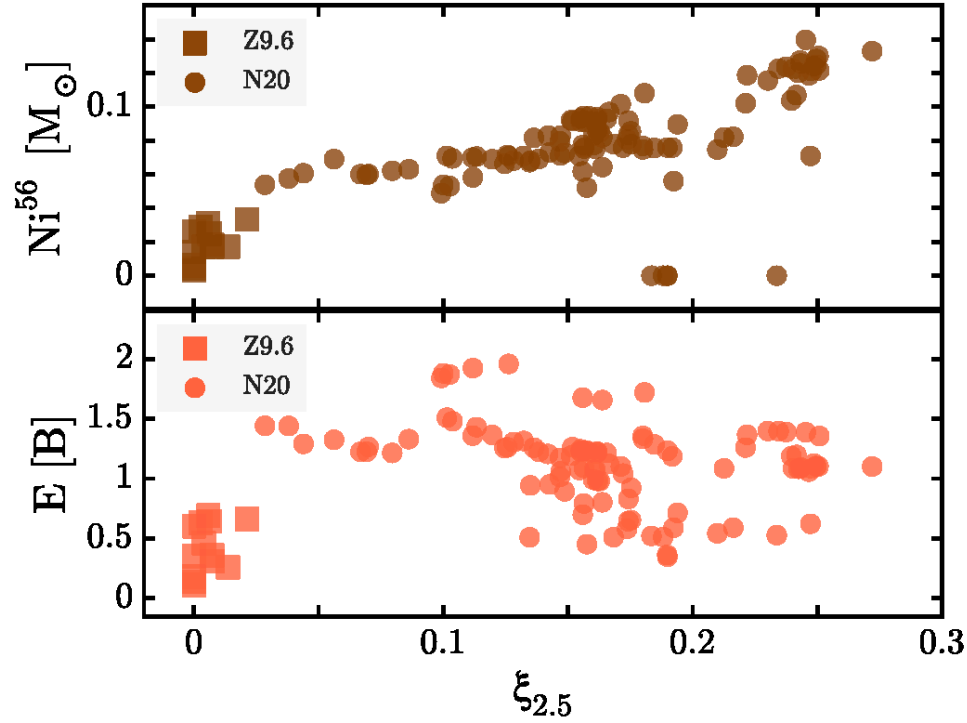


**Table 6**  
 Integrated Statistics (see Section 6.4 for Descriptions; All Masses in  $M_{\odot}$ )

Cal.	$\bar{E}$ (erg)	$\bar{M}_b$	$\bar{M}_g$	Lower $\bar{M}_{\text{BH}}$	Upper $\bar{M}_{\text{BH}}$	$\bar{M}_{\text{Ni}, l}$	$\bar{M}_{\text{Ni}, u}$	SN%	(>12)	(>20)	(>30)
W15.0	0.68	1.55	1.40	8.40	13.3	0.040	0.049	66	47	8	2
W18.0	0.72	1.56	1.40	9.05	13.6	0.043	0.053	67	48	9	2
W20.0	0.65	1.54	1.38	7.69	13.2	0.036	0.044	55	37	3	0
N20.0	0.81	1.56	1.41	9.23	13.8	0.047	0.062	74	52	13	5



## Survey

$Z = 0$ ; 10 to 100  $M_{\odot}$

(Heger & Woosley, 2010, *ApJ*, 724, 341)

Big Bang initial composition, Fields (2002), 75% H, 25% He

10–12  $M_{\odot}$   $\Delta M = 0.1 M_{\odot}$

12–17  $M_{\odot}$   $\Delta M = 0.2 M_{\odot}$

17 - 19  $M_{\odot}$   $\Delta M = 0.1 M_{\odot}$

19–20  $M_{\odot}$   $\Delta M = 0.2 M_{\odot}$

20 - 35  $M_{\odot}$   $\Delta M = 0.5 M_{\odot}$

35 - 50  $M_{\odot}$   $\Delta M = 1 M_{\odot}$

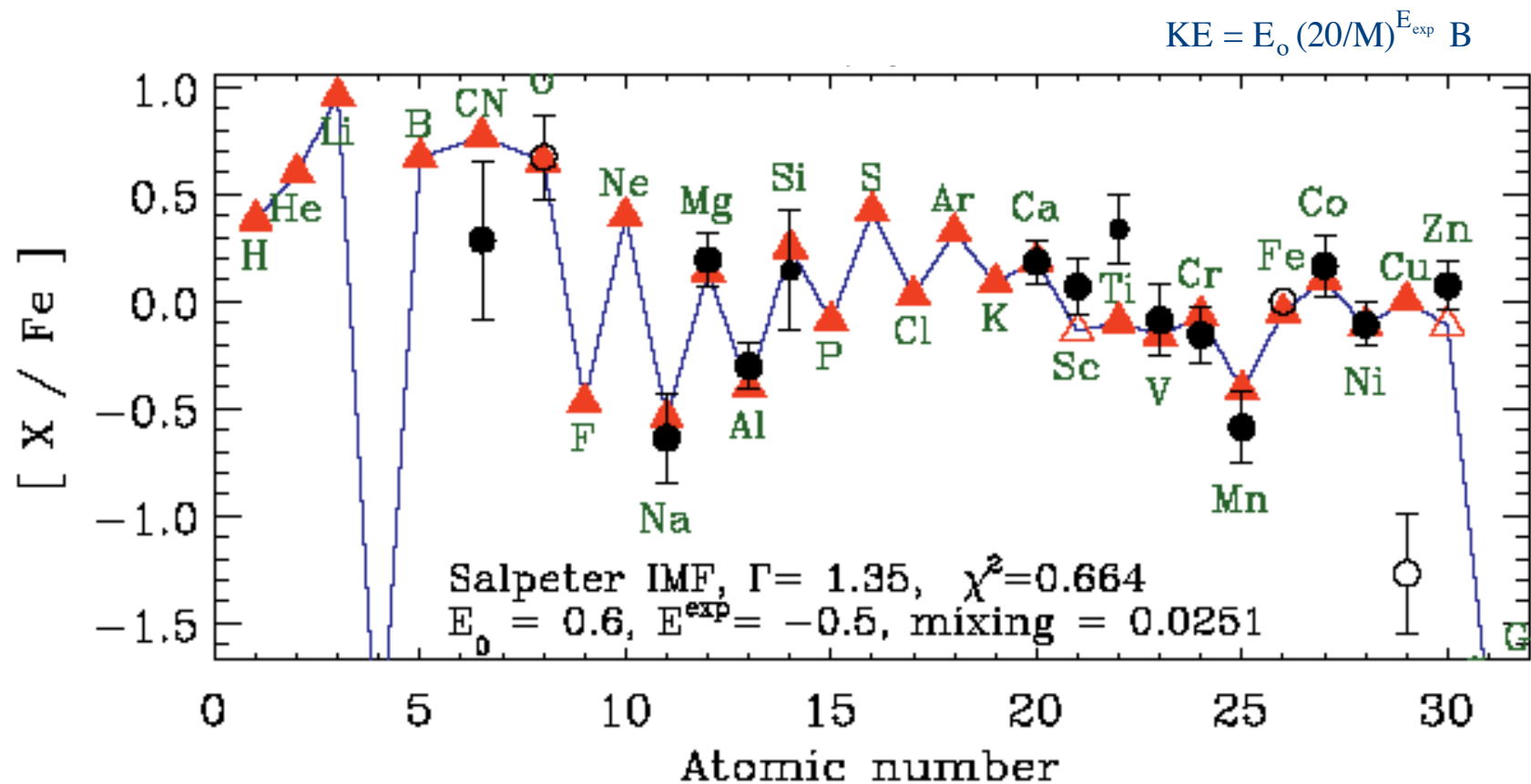
50 - 100  $M_{\odot}$   $\Delta M = 5 M_{\odot}$

Evolved from main sequence to presupernova and then exploded with pistons near the edge of the iron core ( $S/N_{\text{pk}} = 4.0$ )

*Each model exploded with a variety of energies from 0.3 to  $10 \times 10^{51}$  erg.*

126 Models  
at least 1000 supernovae

Integrated yield of 126 masses 11 - 100  $M_{\odot}$  (1200 SN models), with  $Z=0$ , Heger and Woosley (2008, ApJ 2010) compared with low Z observations by Lai et al (*ApJ*, 681, 1524, (2008)). Odd-even effect due to sensitivity of neutron excess to metallicity and secondary nature of the s-process.



Cr I and II, non-LTE effects; see also Sobeck et al (2007)

28 metal poor stars in the Milky Way Galaxy  
 $-4 < [\text{Fe}/\text{H}] < -2$ ; 13 are  $< -2.6$

## MISSING PIECES

- ${}^6\text{Li}$ ,  ${}^9\text{Be}$ ,  ${}^{10}\text{B}$ , part of  ${}^7\text{Li}$   
Cosmic ray spallation, some  ${}^7\text{Li}$  from AGB
- ${}^{15}\text{N}$  and now  ${}^{17}\text{O}$   
Classical Novae
- ${}^{43}\text{Ca}$ ?, part of  ${}^{44}\text{Ca}$ ,  ${}^{47}\text{Ti}$ , part of  ${}^{51}\text{V}$   
Helium detonation Type Ia supernovae
- ${}^{48}\text{Ca}$ ,  ${}^{50}\text{Ti}$ ,  ${}^{54}\text{Cr}$ , ( ${}^{58,60}\text{Fe}$ ,  ${}^{66}\text{Zn}$  in grains)  
Chandrasekhar Mass Type Ia supernovae
- ${}^{64}\text{Zn}$ ,  ${}^{70}\text{Ge}$ ,  ${}^{74}\text{Se}$ ,  ${}^{78}\text{Kr}$ ,  ${}^{84,88}\text{Sr}$ ,  ${}^{89}\text{Y}$ ,  ${}^{90}\text{Zr}$ ,  ${}^{92}\text{Mo}$ ?  
Neutrino driven winds from neutron stars

## NUCLEOSYNTHESIS IN NEUTRON-RICH SUPERNOVA EJECTA<sup>1</sup>

D. HARTMANN,<sup>2,3</sup> S. E. WOOLLEY,<sup>2,4</sup> AND M. F. EL EID<sup>3,7</sup>

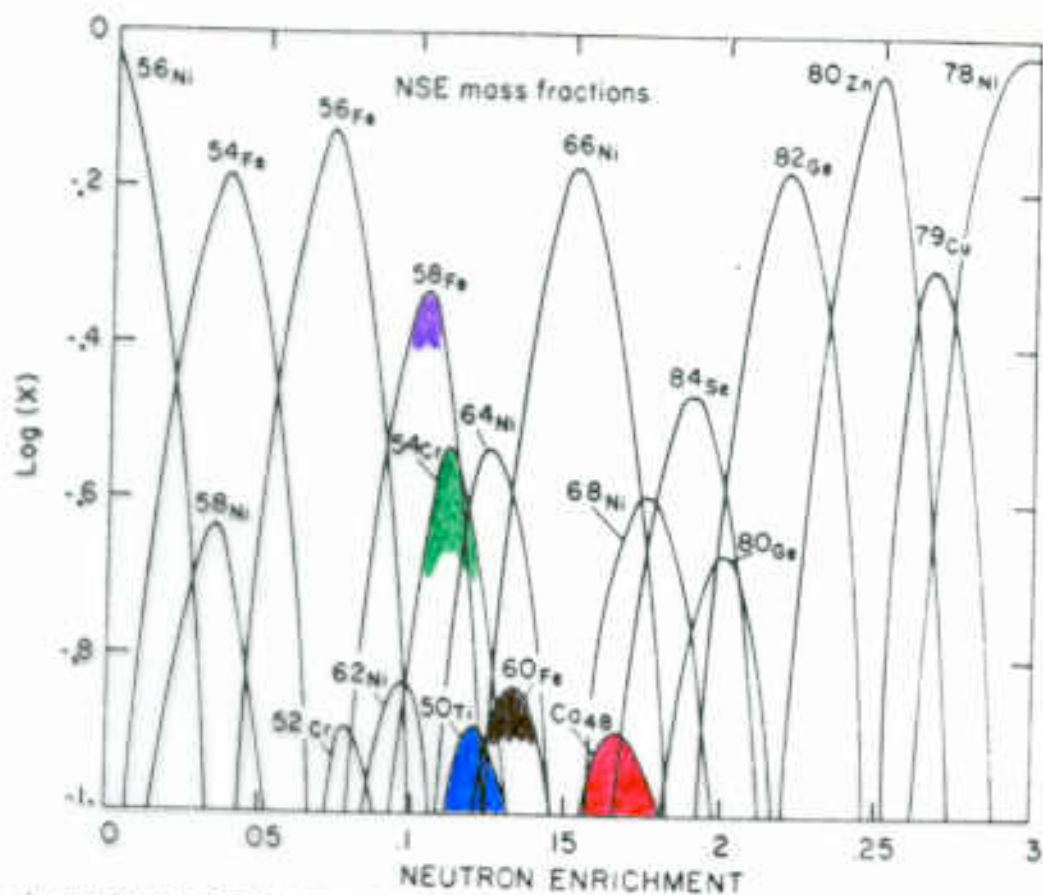
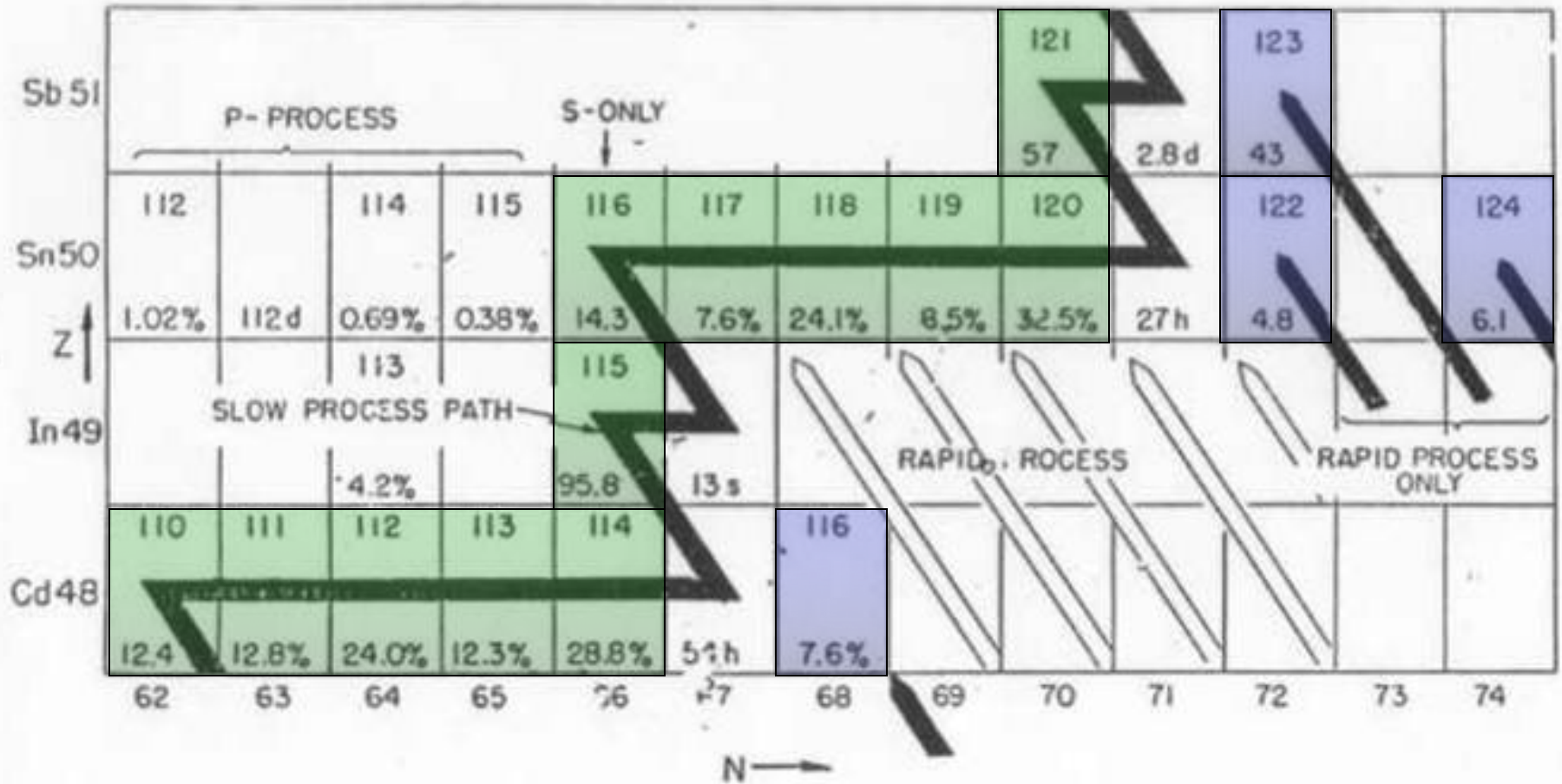


FIG. 2.—Mass fractions obtained in NSE as a function of neutron enrichment  $\eta$  for fixed temperature  $T = 3.5 \times 10^9$  K and density  $\rho = 10^7$  g cm<sup>-3</sup>.

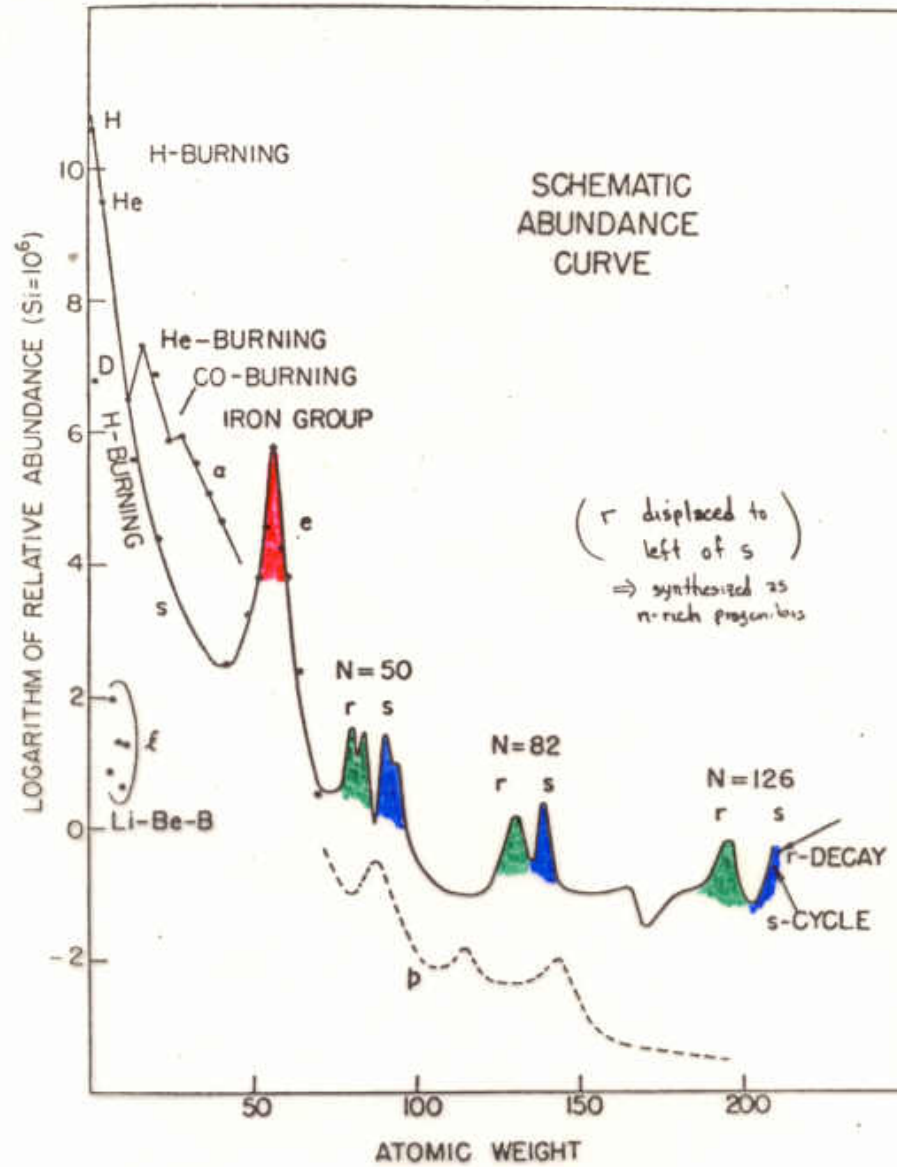
# *The r-Process*

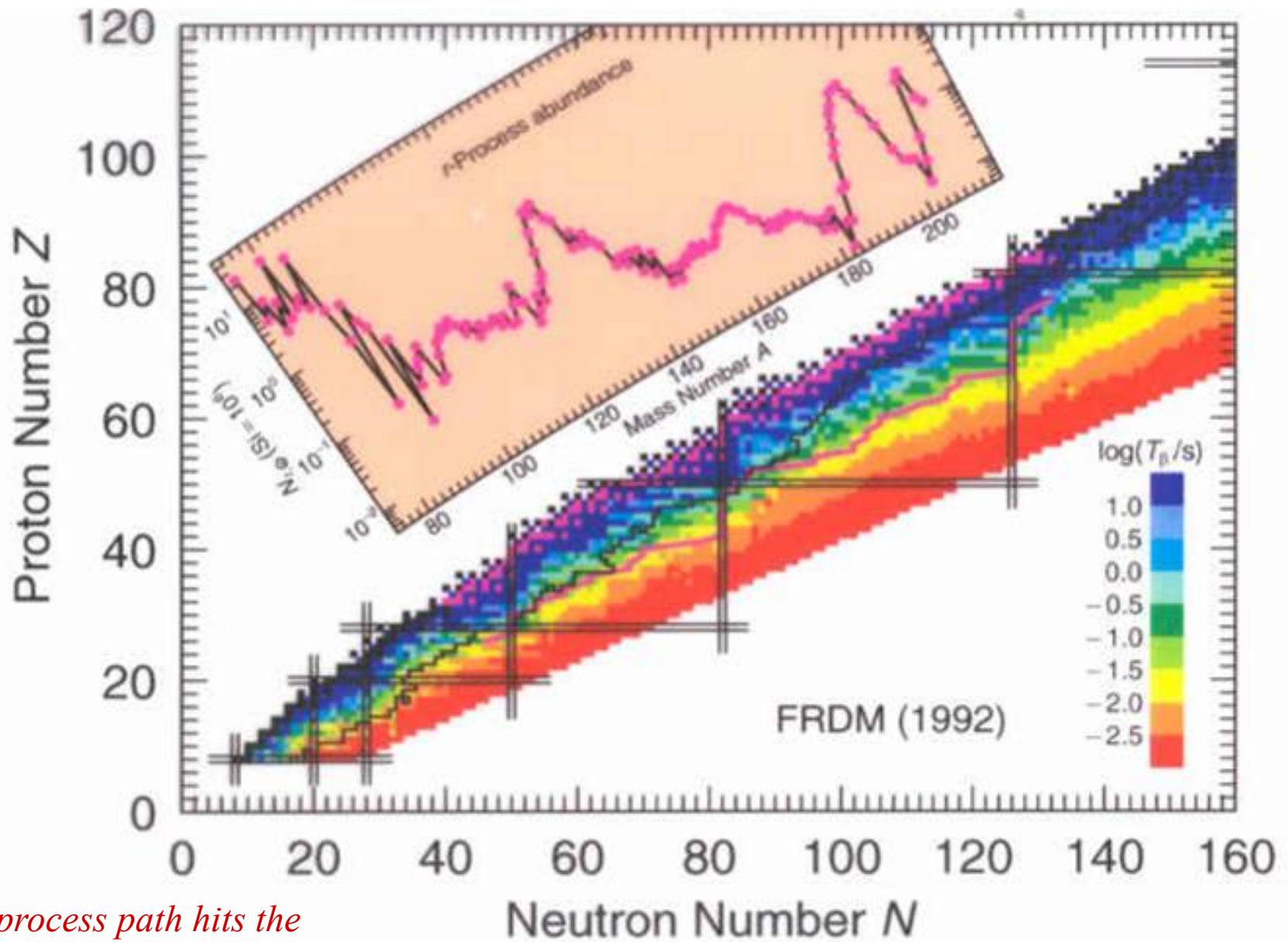
*The rapid addition of neutrons to iron group nuclei that produces the most neutron-rich isotopes up to uranium and beyond. This is thought to occur either in the deepest ejecta of supernovae or in merging neutron stars.*

# The *r*-Process



# The r-Process





*The r-process path hits the closed neutron shells for a smaller value of  $A$  (i.e., a lower  $Z$ )*

These heavy nuclei cannot be made by the s-process, nor can they be made by charged particle capture or photodisintegration.

Photodisintegration would destroy them and make p-nuclei. The temperatures required for charged particle capture would destroy them by photodisintegration.

Their very existence is the proof of the addition of neutrons on a rapid, explosive time scale. This requires a high density of neutrons.

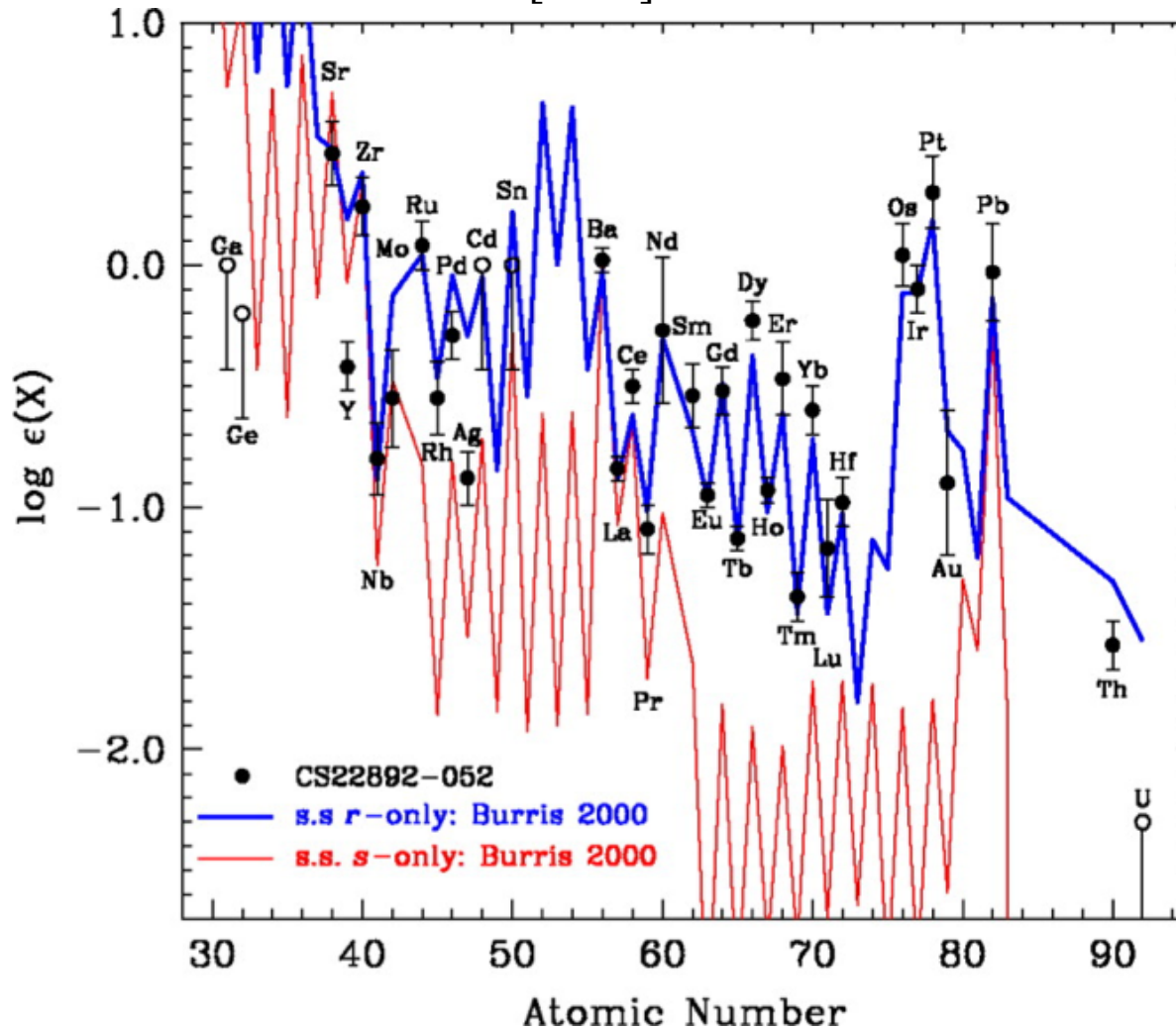
They were once attributed to the Big Bang (Gamow 1946), but we now know the density is far too low.

Still, observations suggest though that the r-process arose or at least began to be produced very early in the universe, long before the s-process.

# CS 22892-052

Snedden et al, ApJ, 591, 936 (2003)

[Fe/H]  $\sim$  -3.1



If neutrons are to produce the r-process nuclei then  $\beta$ -decay must be responsible for the increase in proton number along the r-process path. Protons would combine with neutrons and end up in helium.

The neutron density must be high both because the abundances themselves indicate a path that is very neutron-rich (so  $\rho Y_n \lambda_{n\gamma}$  must be  $\gg 1/\tau_\beta$  near the valley of  $\beta$ -stability) and because only very neutron-rich nuclei have sufficiently short  $\beta$ -decay lifetimes to decay and reach, e.g., Uranium, before  $Y_n$  goes away ( $\tau_{HD}$ ) in any realistic scenario.

The beta decay lifetimes of nuclei that are neutron-rich become increasingly short because of the large Q-value for decay:

- More states to make transitions to. Greater likelihood that some of them have favorable spins and parities
- Phase space – the lifetime goes roughly as the available energy to the fifth power

We shall find that the typical time for the total r-process is just a few seconds. Neutron rich nuclei have smaller neutron capture cross sections because  $Q_{n\gamma}$  decreases, eventually approaching zero

$t < 1 \text{ s} \Rightarrow$  Take  $\lambda_{n\gamma} \sim 10^4$ . One needs  $\rho Y_n \lambda_{n\gamma} \gg 1$ . for many captures to happen in a second

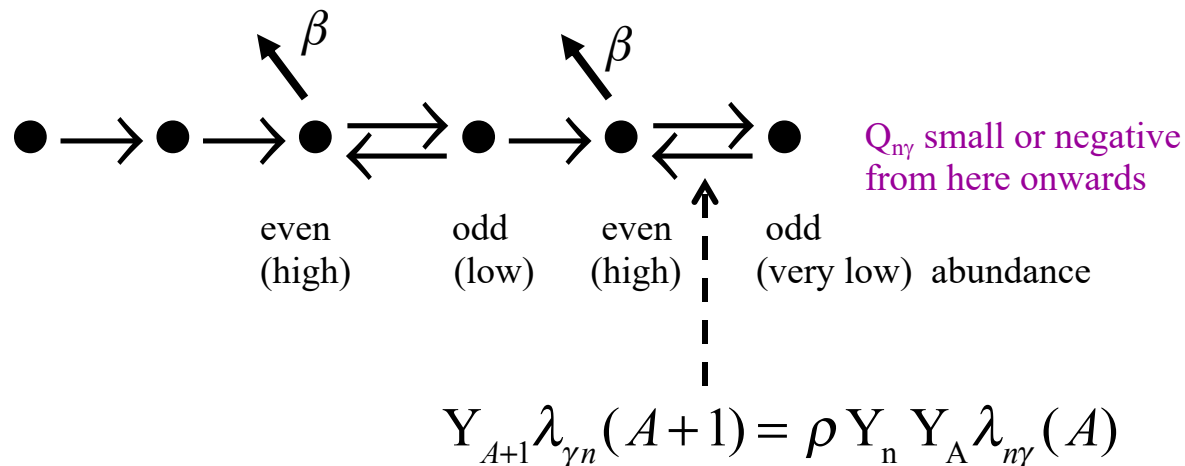
This implies that  $n_n = \rho N_A Y_n \gg \frac{N_A}{\lambda_{n\gamma}} \sim 10^{20} \text{ cm}^{-3}$   $\frac{1}{Y_A} \left( \frac{dY_A}{dt} \right) = \rho Y_n \lambda_{n\gamma}$

For such large neutron densities neutron capture will go to the (T-dependent) neutron drip line and await a beta decay.

# How it works

The r-process proceeds by rapidly capturing neutrons while keeping  $Z$  constant, until a "waiting point" is reached. At the waiting point(s), photo-neutron ejection (photodisintegration) balances neutron capture. At zero temperature, the waiting point would be the neutron drip line ( $S_n \leq 0$ ), but the r-process actually happens at high temperature (a necessary condition to obtain the high neutron density).

At the waiting point (or points), beta decay eventually happens creating  $Z+1$ . Neutron capture continues for that new element until a new waiting point is found.



The temperature cannot be too high or

- The heavy isotopes will be destroyed by photo-disintegration
- $(\gamma, n)$  will balance  $(n, \gamma)$  too close to the valley of  $\beta$  stability where  $\tau_\beta$  is long

At a waiting point for a given Z:

$$\frac{Y_{A+1}}{Y_A} = \rho Y_n \frac{\lambda_{n\gamma}(A)}{\lambda_{\gamma n}(A+1)} \quad A + n \xrightleftharpoons[\gamma]{} A + 1$$

$$= \rho Y_n \left(9.89 \times 10^9\right)^{-1} \frac{G(A+1)}{G(A)} T_9^{-3/2} \frac{(A+1)}{A} \exp(11.6045 Q_{n\gamma} / T_9)$$

At a waiting point photodisintegration will give  $Y_{A+1}$  and  $Y_A$  comparable abundances – at least compared with abundances far from A. Since we only care about log's anyway ...

Ignoring  $G'$  s and other less dominant terms

$$\log \frac{Y_{A+1}}{Y_A} \sim 0 \sim \log \rho Y_n - 10 + 5.04 Q_{n\gamma} / T_9$$

---



---

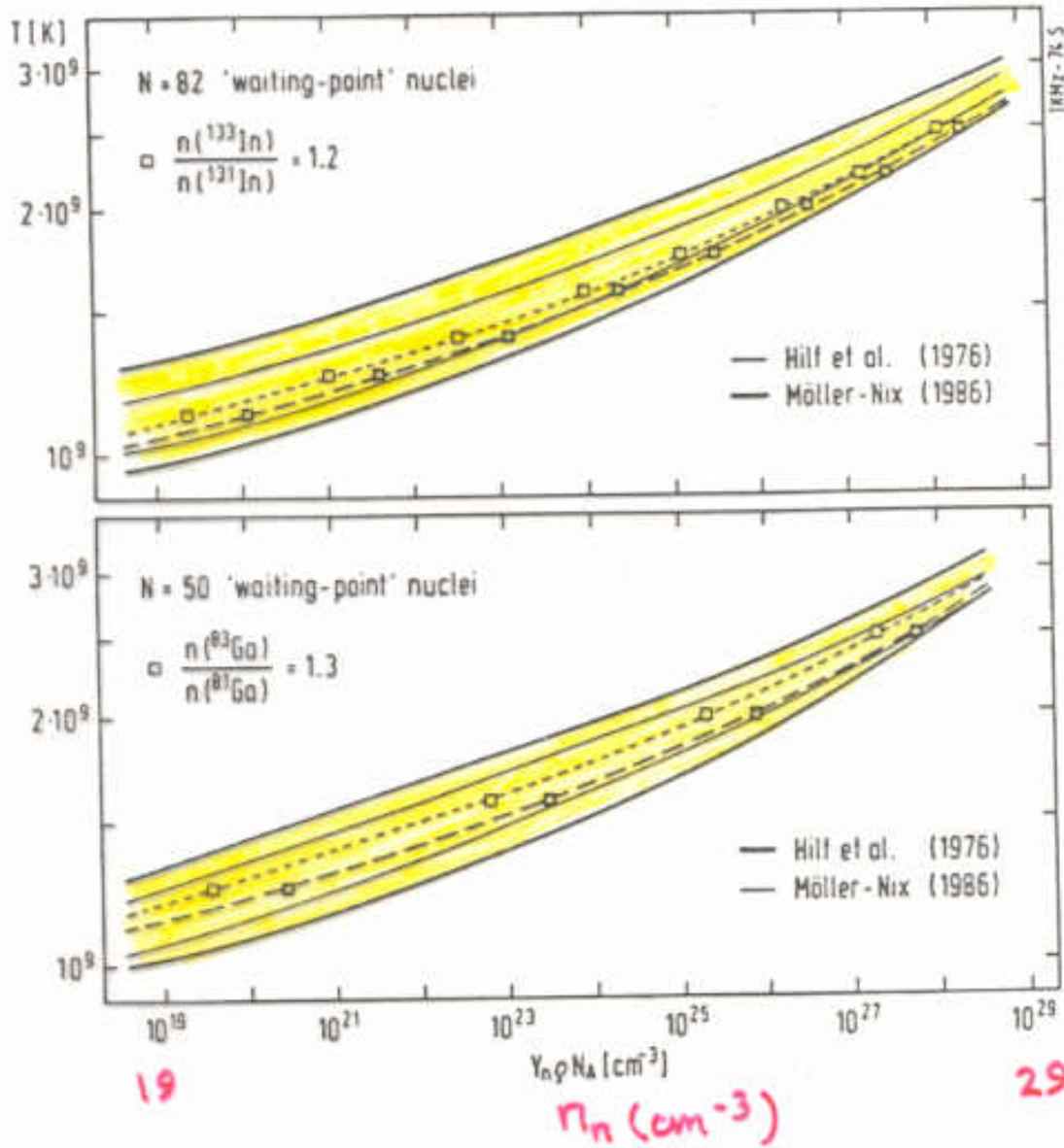
$\rho Y_n$	$T_9$	$Q_{\text{lim}}(\text{MeV})$
1 gm cm <sup>-3</sup>	1	1.98
	2	3.97
	3	5.94
10 <sup>3</sup> gm cm <sup>-3</sup>	1	1.39
	2	2.78
	3	4.17

---

Therefore the path of the r-process ( $Q_{\text{lim}}$ ) depends upon a combination of  $T_9$  and  $n_n$ . Actually both are functions of the time.

# Optimal conditions for the r-process

T



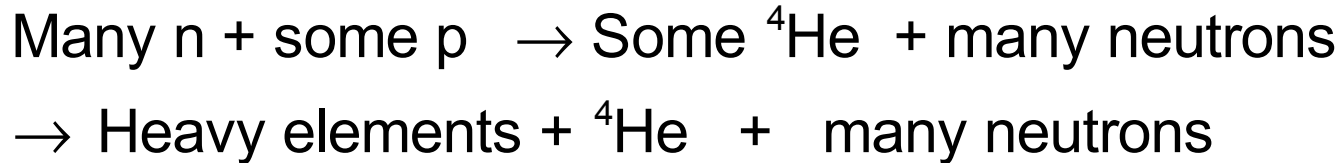
*Based upon estimated lifetimes and  $Q$ -values along path of the r-process.*

Kratz et al. (1988)

For example, at  $T_9=2.5$ ,  
 $n_n = \rho N_A Y_n \sim 10^{27} \text{ cm}^{-3}$   
 or  $\rho Y_n \sim 10^3$ .

## Sites for the r-process:

All modern scenarios for making the r-process achieve a very large density of neutrons and a very high neutron-to-seed ratio by invoking an explosive event in which the matter is, at least briefly, in the form of nucleons – neutrons and protons – with a large excess of neutrons. The ensuing nucleosynthesis then resembles a dense, neutron-rich Big Bang.

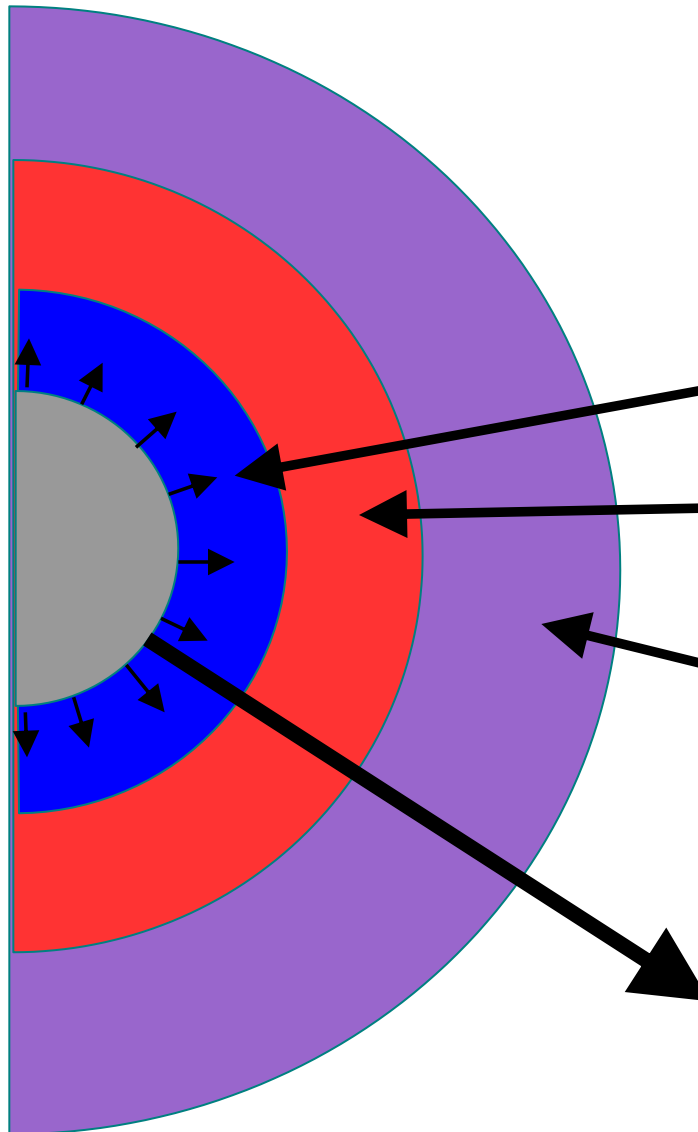


This last step would not happen at Big Bang densities but happens in a stellar environment where the density is enormously greater.

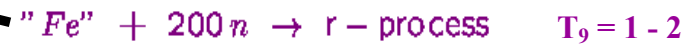
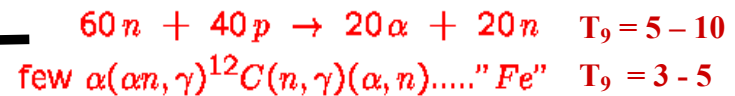
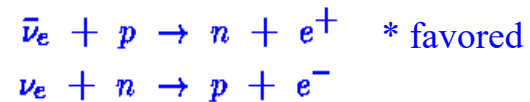
Three sites have been discussed in the last decade :

- Neutrino-powered winds from proto-neutron stars
- Merging neutron stars and neutron stars merging with black holes
- Dense accretion disks around black holes (could be an outcome of merging neutron stars)

# r-Process Site #1: The Neutrino-powered Wind \*

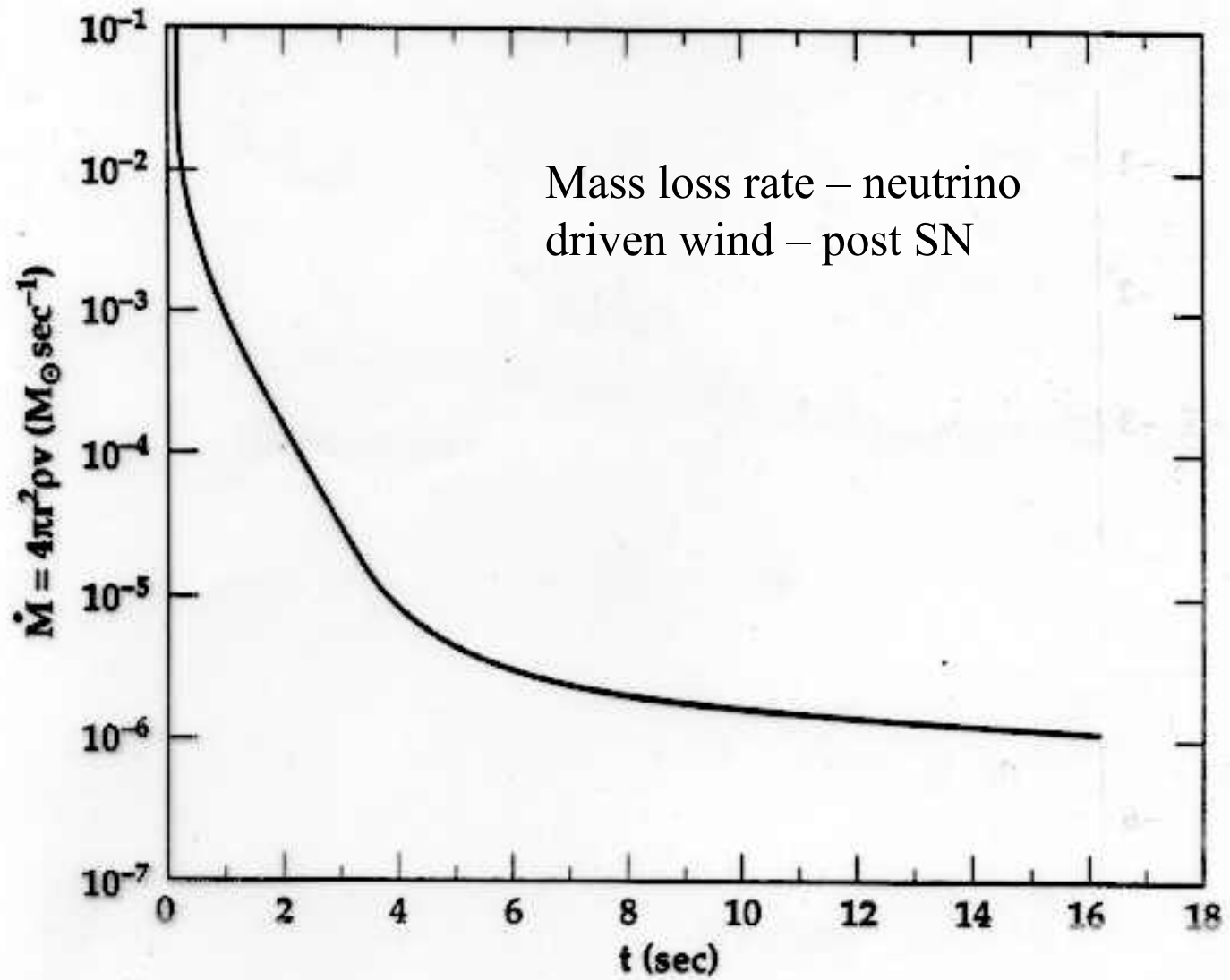


Anti-neutrinos are "hotter" than the neutrinos, thus weak equilibrium implies an appreciable neutron excess, typically 60% neutrons, 40% protons



e.g., 5% by mass "Fe"  
and 20% by mass neutrons  
( $Y_e = 0.4$ ) implies 200 neutrons  
per iron. The other 75% is alphas.

Nucleonic wind, 1 - 10 seconds



## WHAT SETS $Y_e$ IN THE WIND?

(Qian et al. 1993)

$$Y_e = \frac{X_p}{X_n + X_p}$$

$$\frac{dX_n}{dt} = X_p(\lambda_{\bar{\nu}}(p) + \lambda_e(p)) - X_n(\lambda_{\nu}(n) + \lambda_{e^+}(n))$$

$$\frac{dX_p}{dt} = -X_p(\lambda_{\bar{\nu}}(p) + \lambda_e(p)) + X_n(\lambda_{\nu}(n) + \lambda_{e^+}(n))$$

So long as the fluxes (and spectra) of  $\nu$  and  $\bar{\nu}$  are equal, the neutron-proton mass difference negligible, the electrons non-degenerate, and the number of positrons equal to the number of electrons,  $Y_e$  will be 0.50.

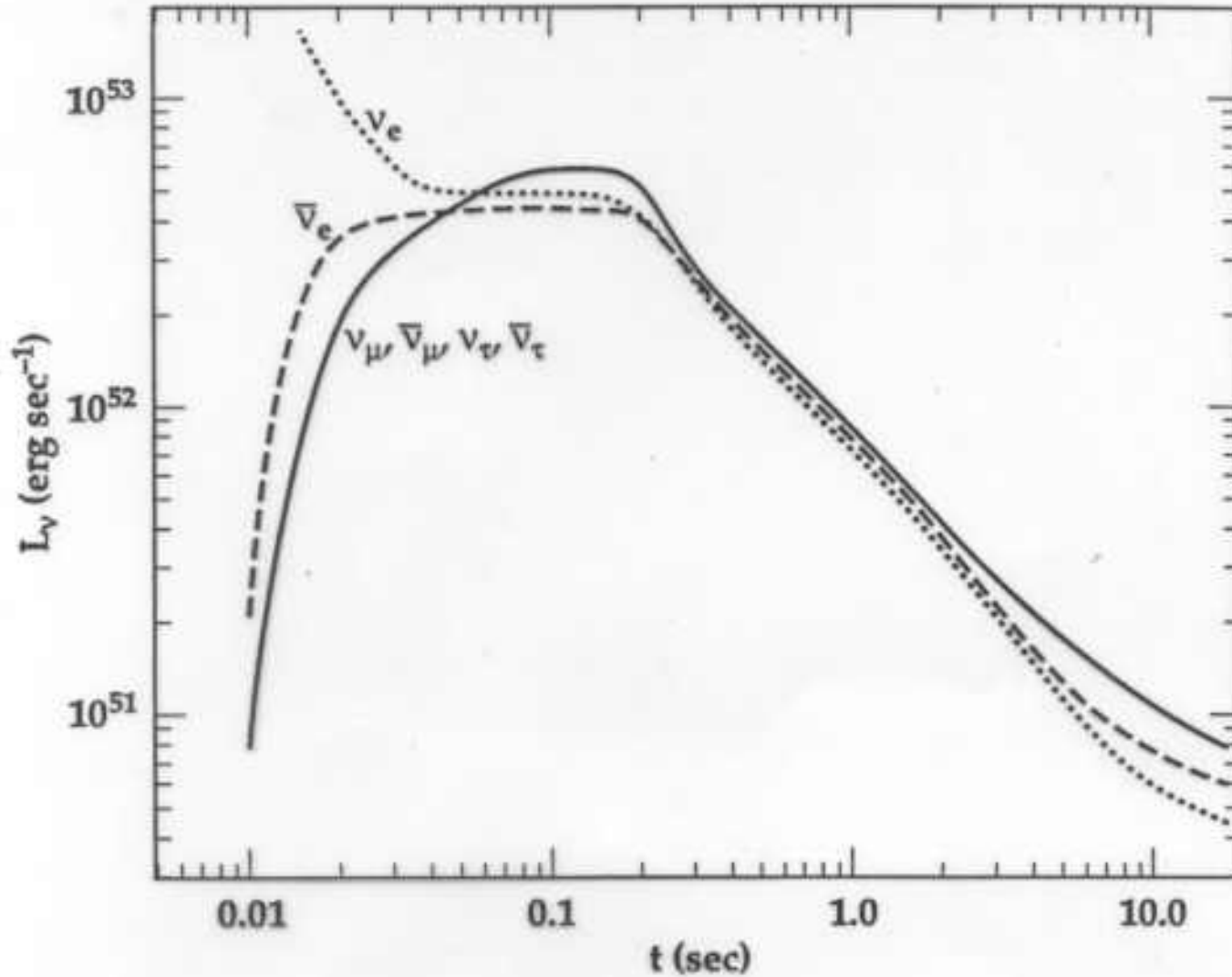
Of these the neutrino interactions predominate (it takes many such interactions to lift a proton from the neutron star).

$$Y_e \approx \frac{\lambda_{\nu}(n)}{\lambda_{\bar{\nu}}(p) + \lambda_{\nu}(n)}$$

(which is less than 0.5 if  $\lambda_{\bar{\nu}}(p) > \lambda_{\nu}(n)$ .)

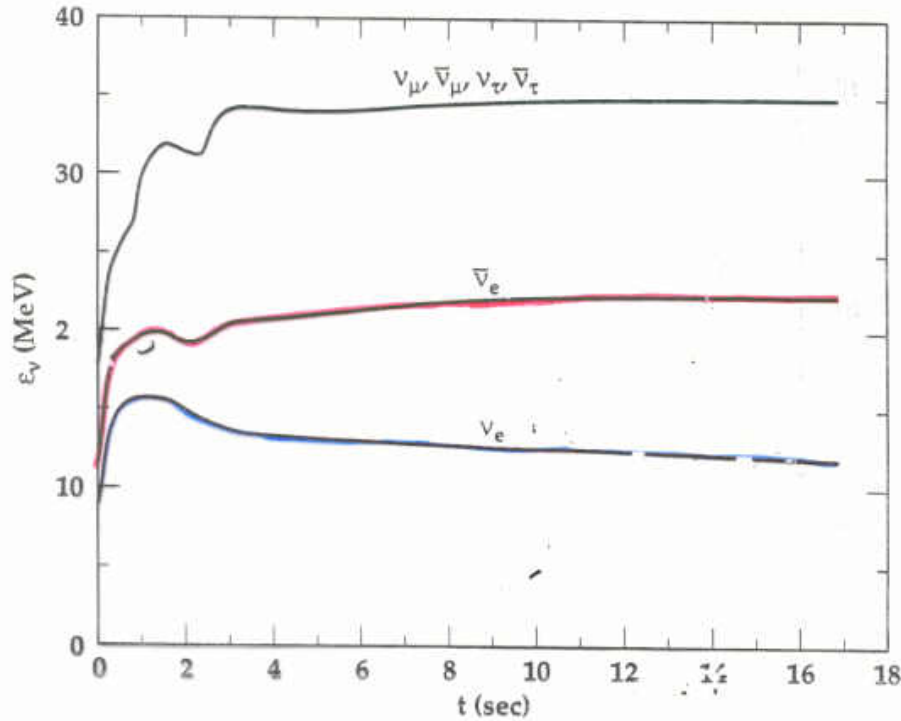
After 0.1 s, the luminosities of all flavors of neutrinos are equal - made by pair annihilation

Woosley et al  
ApJ, 433, 229  
(1994)



But the average energy each flavor of neutrino is not the same

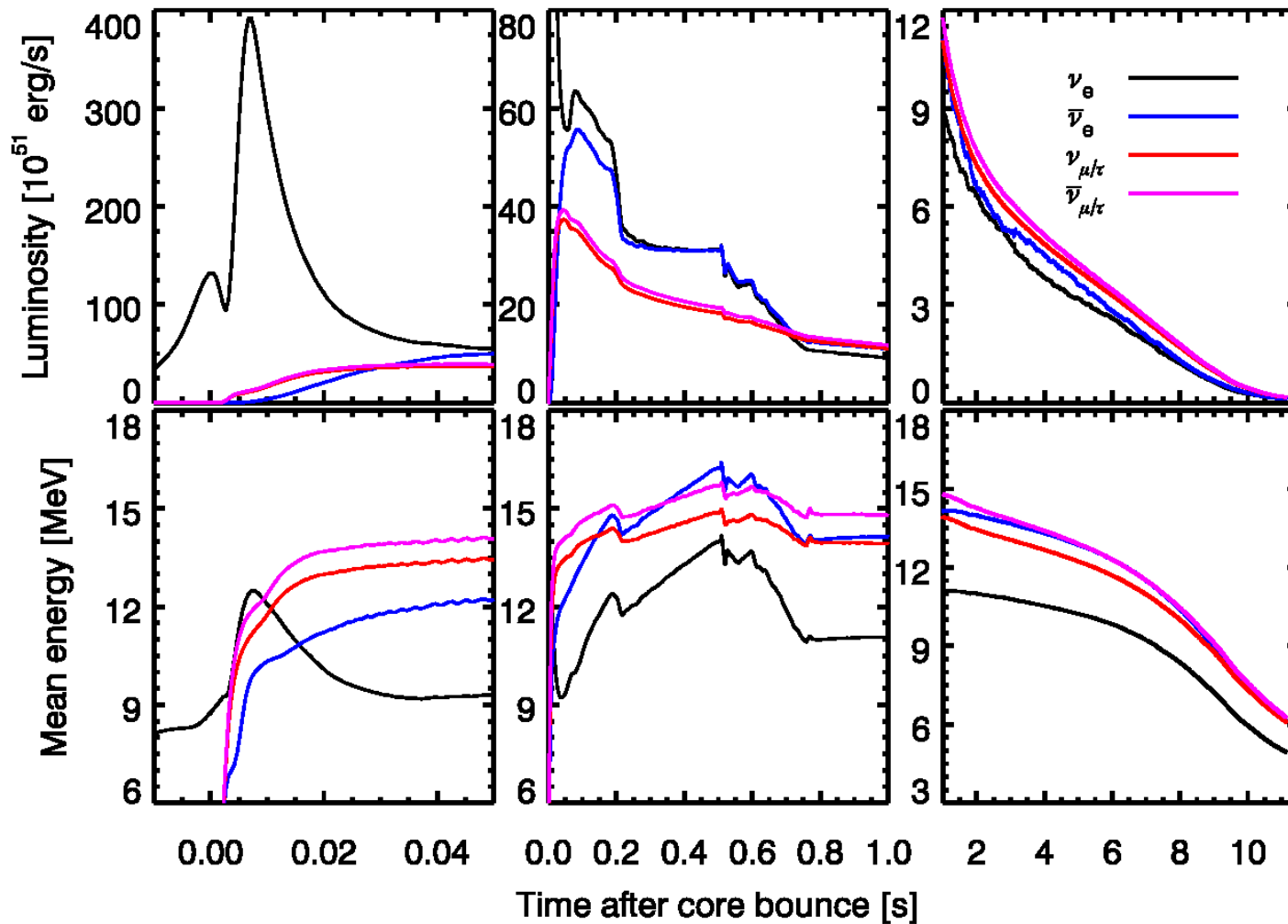
$Y_e$  decreases with time.



Wilson (1994)

$t$ (sec)	$Y_e$ in wind	$Y_e \equiv \sum \frac{Z_i X_i}{A_i}$
0.30	0.489	
1.05	0.488	
5.85	0.474	
9.69	0.429	
15.08	0.365	

$X_n$  (nsec)  $\approx 1 - 2Y_e$   
 ( $h_i T$  /  $2.1 \text{ MeV}$ ) rest ...  
 Fig. 3  $X_e$



$T_{\mu\tau}$  not as hot as it used to be

Ratio of electron antineutrino and neutrino temperature also less

## In order for this to work one needs.

1) low  $Y_e$  because  $T_{\bar{\nu}_e} > T_{\nu_e}$

2) High entropy  $S \sim \frac{T^3}{\rho}$  (entropy dominated by radiation)

need  $S \sim 400$

If the density is too high, too many alphas reassemble and the neutron to seed ratio is small

For higher entropy the density is lower at a given temperature. The rates governing the reassembly of  $\alpha$ -particles are proportional to  $\rho^2$  (the  $3\alpha$  reaction) or  $\rho^3$  (the  $\alpha\alpha n$  reaction)

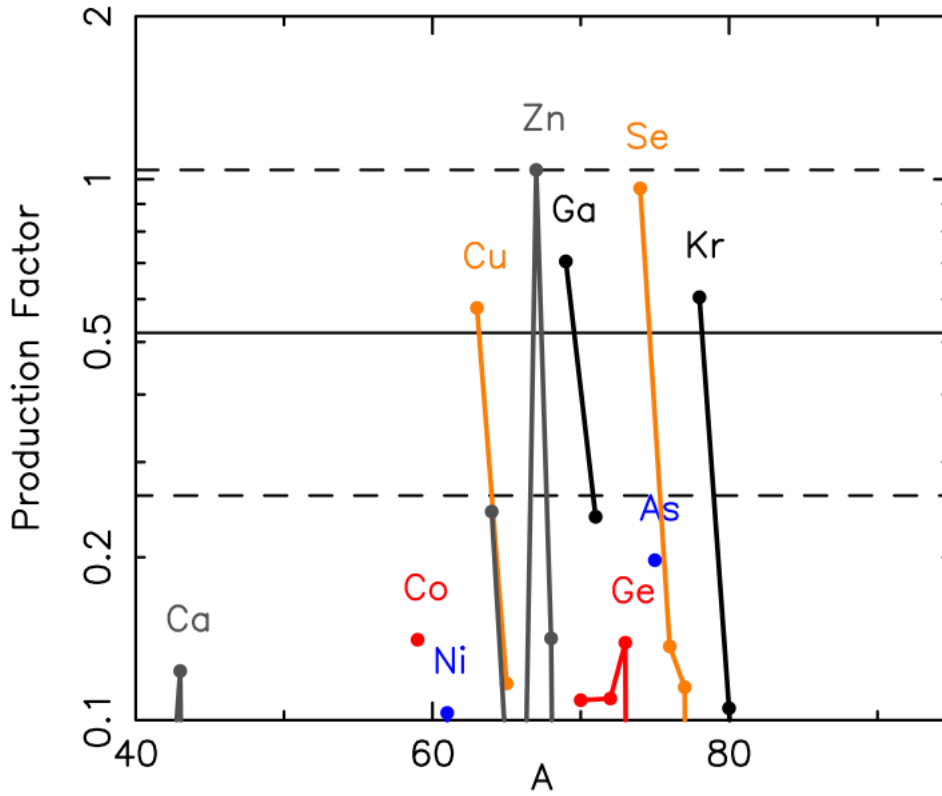
3) Rapid time scale -  $\tau \sim \frac{R}{v_{wind}} \sim 100\text{ms}$ .

Why it hasn't worked so far

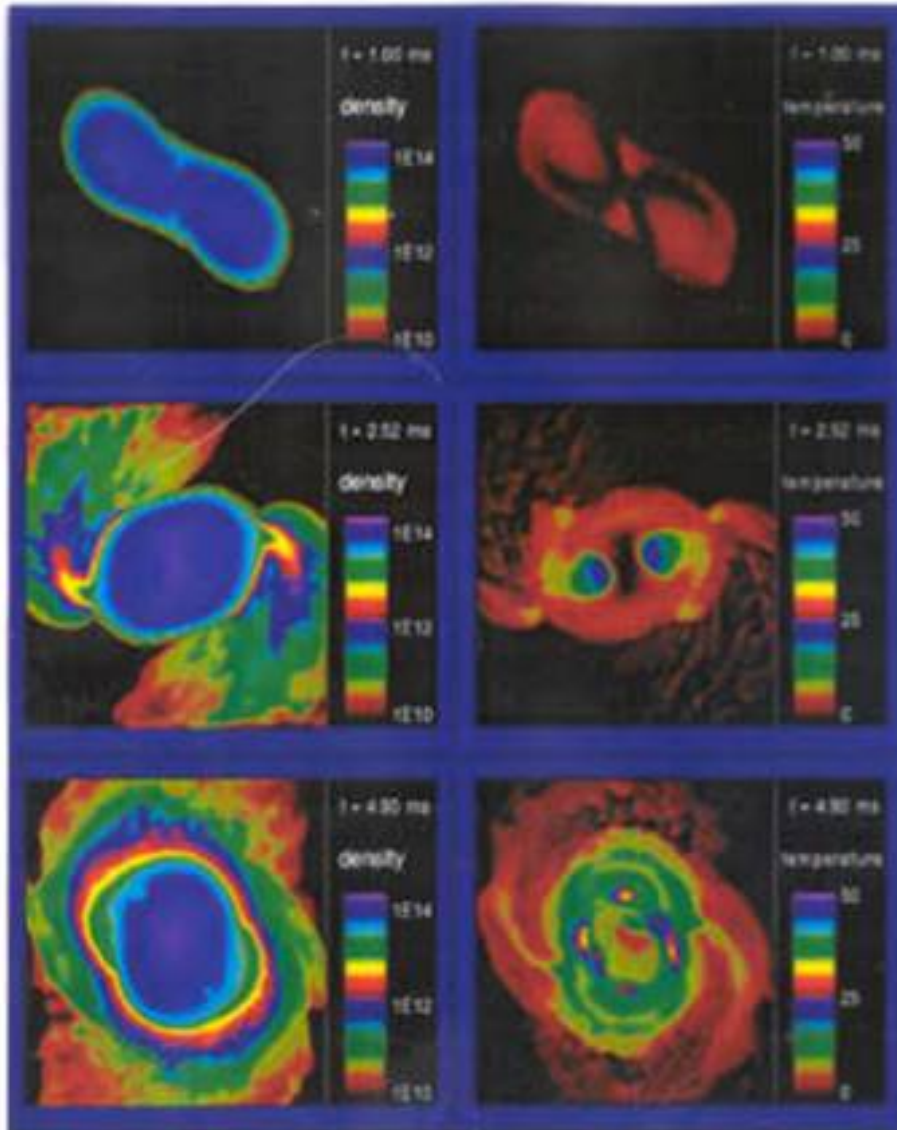
Need entropies  $s_{\text{rad}}/N_A k \sim 400$ . Most calculations give  $\sim 100$ .  
Magnetic fields could help – Thompson 2003, *ApJL*, **585**, L33.

# Neutrino-powered wind

Roberts, Woosley and Hoffman (2010)



## r=Process Site #2 - Merging Neutron Stars



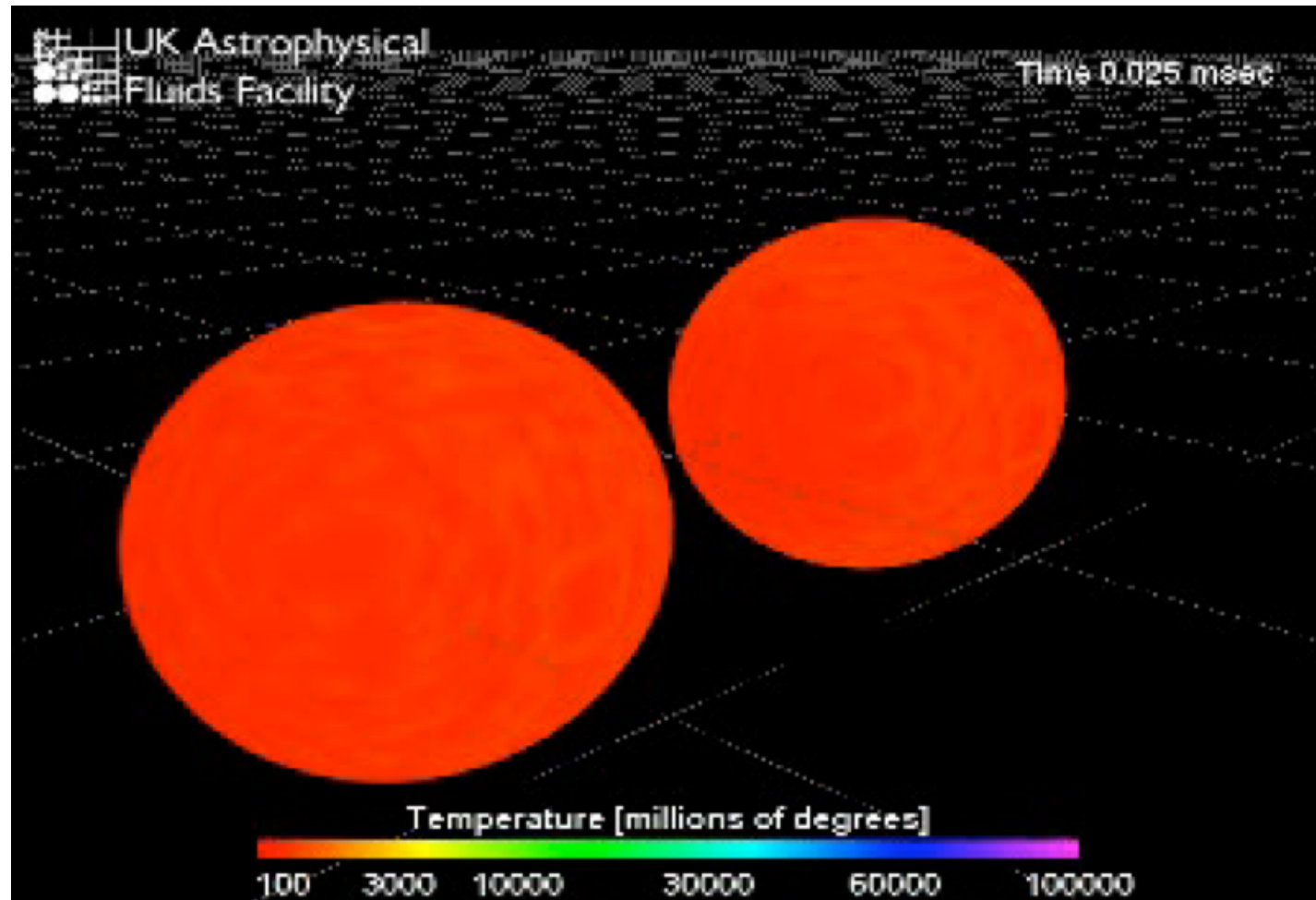
### Merging Neutron Stars:

*May happen roughly once every  $10^5$  years\* in the Milky Way galaxy. Eject 0.01 - 0.1 solar masses of r-process.*

*The currently favored site at least for the heavy r-process*

\* $24 \text{ My}^{-1}$  in the Milky Way  
Chruslinska et al (2017)

Rosswog et al. 2003, *MNRAS*, **345**, 1077 and references therein

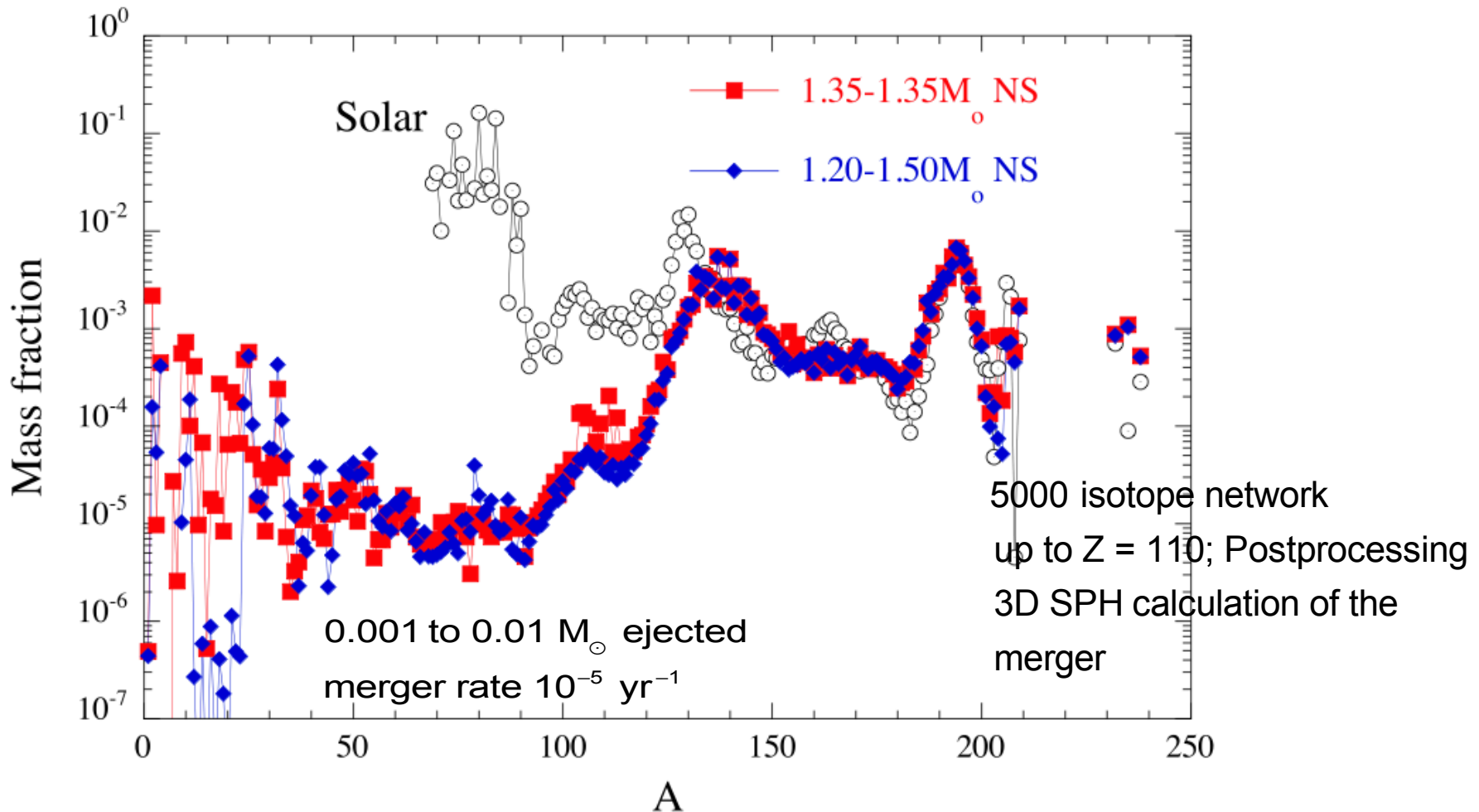


May also jet of neutron rich material after merger

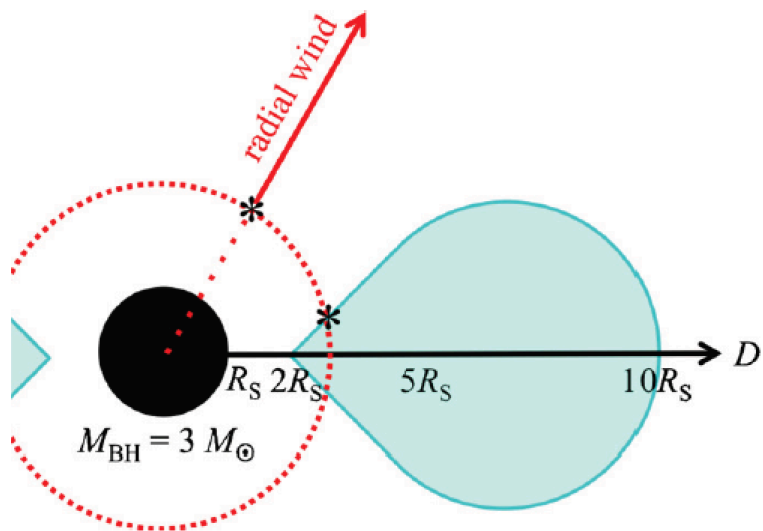
Burrows et al., 2007, *ApJ*, **664**, 416

# Merging neutron stars – r-process nucleosynthesis

Goriely, Bauswein, and Janka (2011)

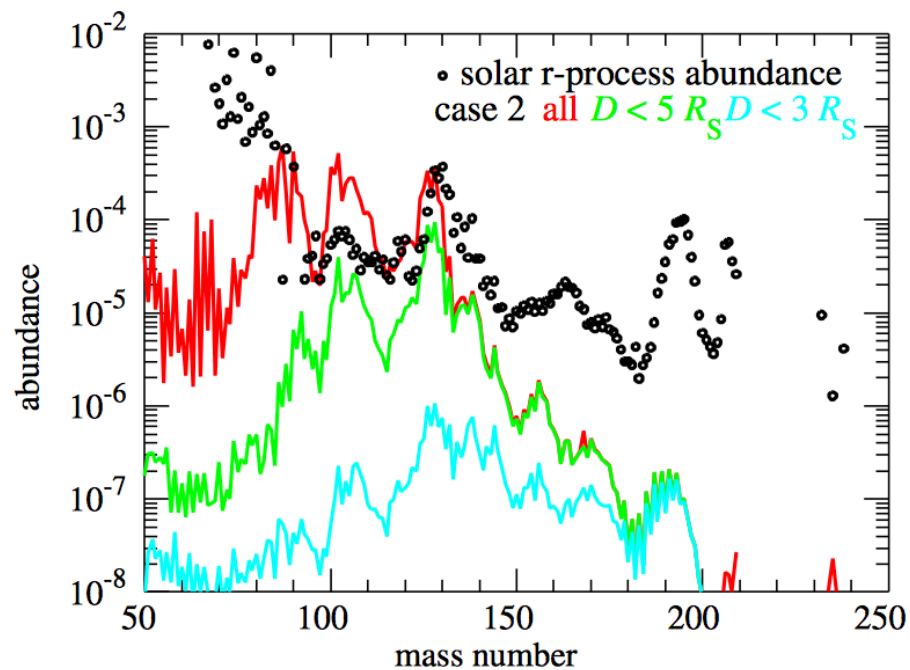
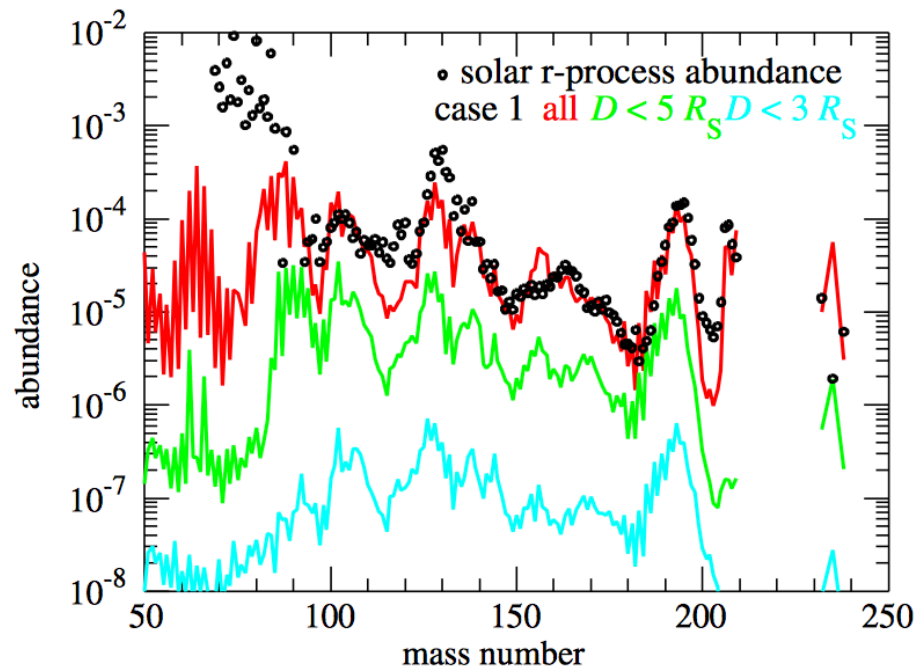


So many neutrons that “fission recycling” occurs leading to a robust pattern that fits the solar abundances above  $A = 110$ . Also need a “weak” r-process site.

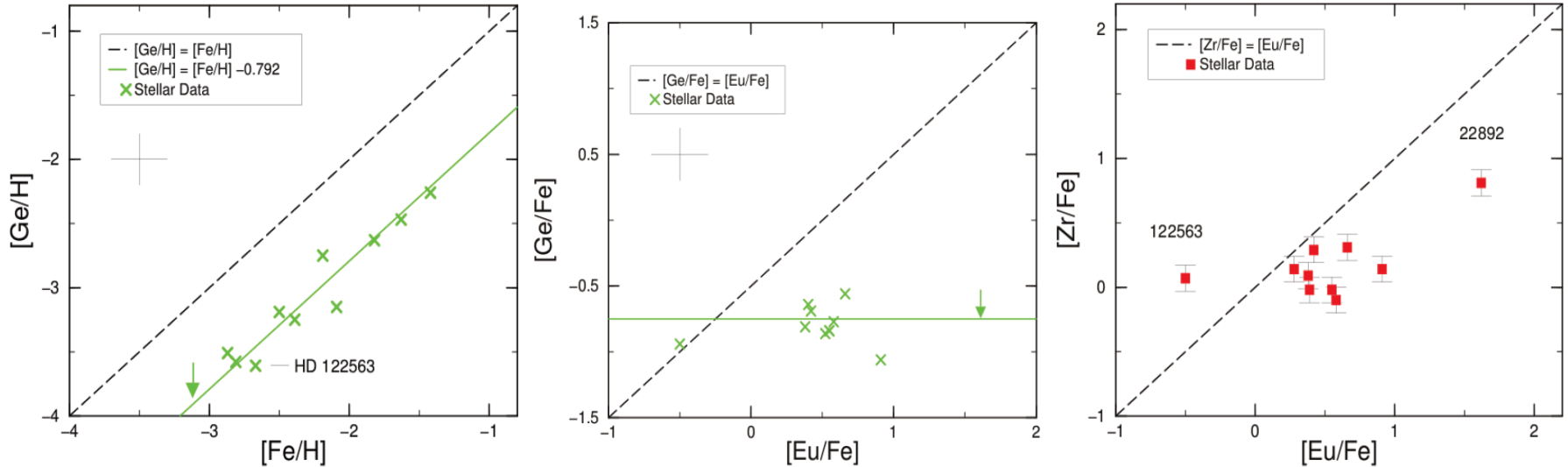


Wanajo and Janka (2012)

*Neutrino-powered wind from  
black hole accretion disk  
following neutron star merger*



## Two r-Processes?



Cowan et al (RMP 2019)

Ge, Zr, and Eu are predominantly r-process elements. At early times Fe is free from SN Ia supernova contributions and is solely a massive star product.

The left frame shows that Ge ( $A = 70 - 76$ ) correlates with iron and is probably a massive star product.

The center frame shows that no such correlation exists between Ge and much heavier Eu ( $A = 151 - 153$ ), suggesting Eu has a different origin

The right frame suggests that Zr (isotopes 90 - 94) is intermediate.

6 *Kasen, Fernández, & Metzger*

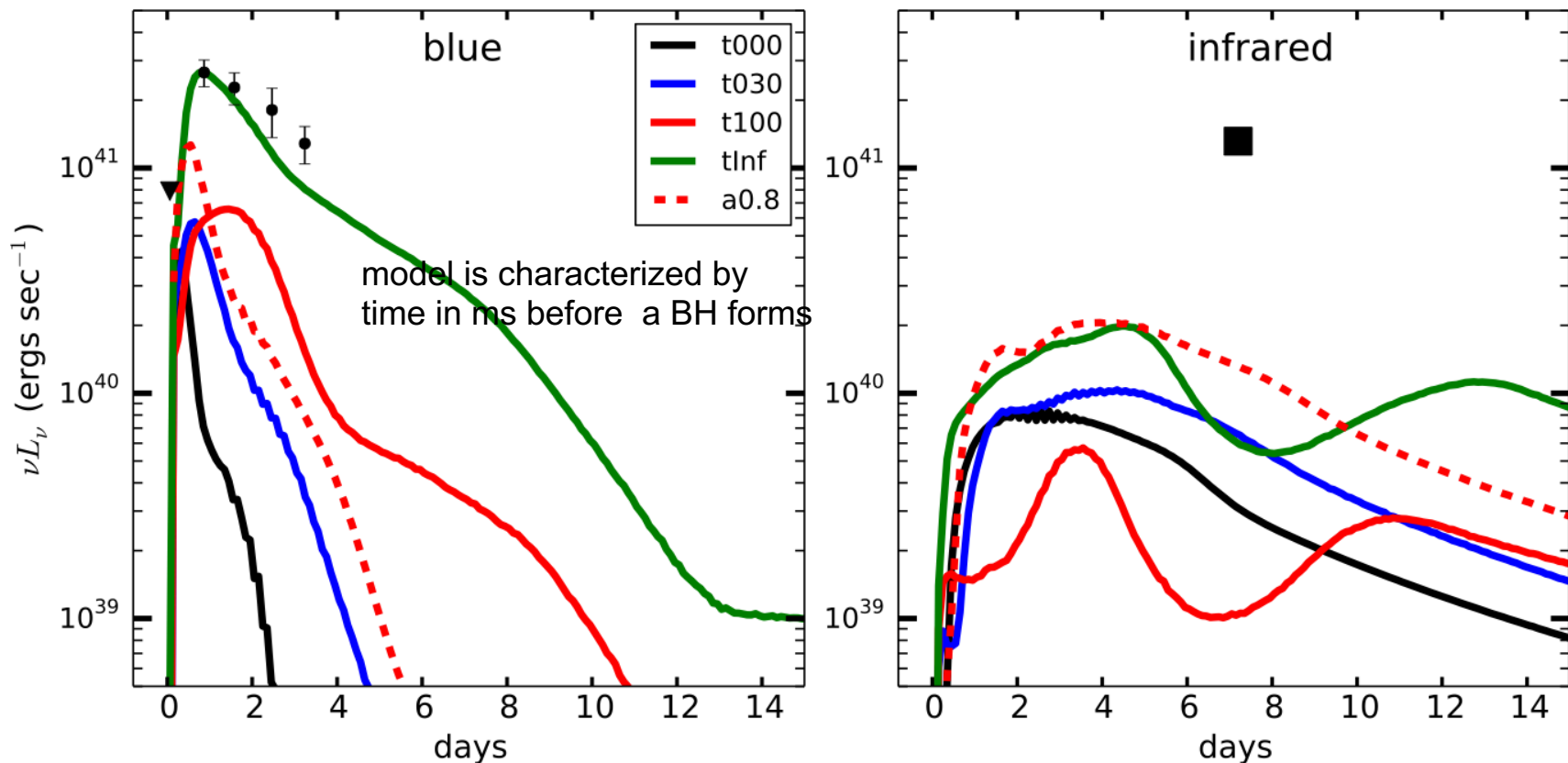
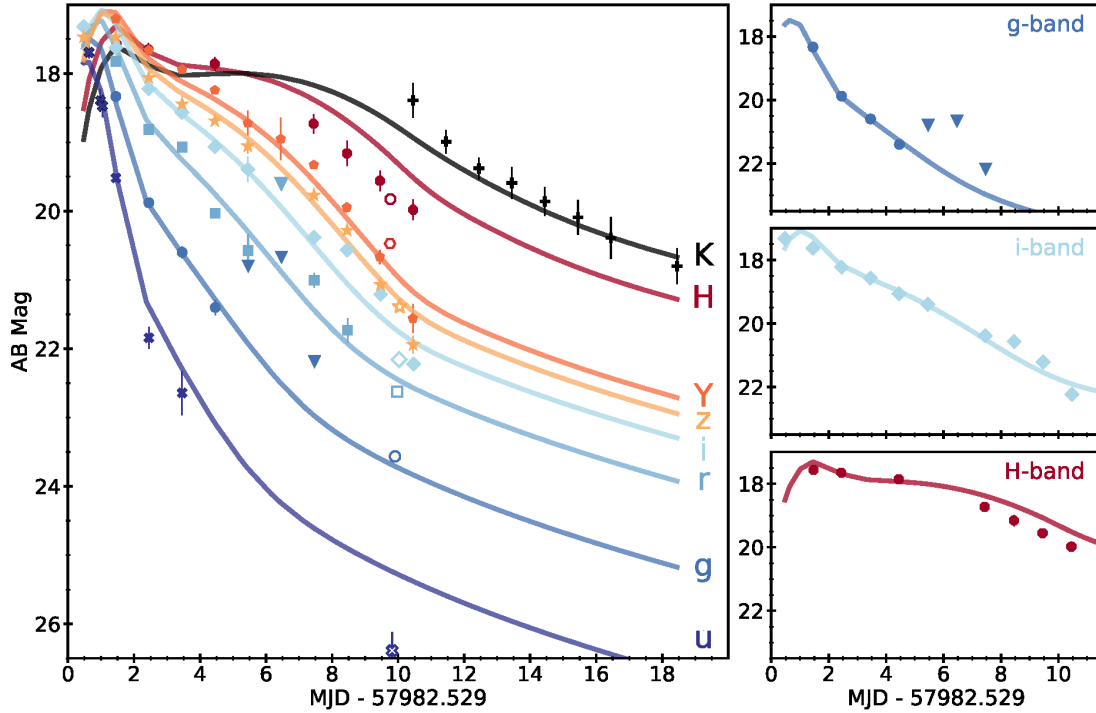


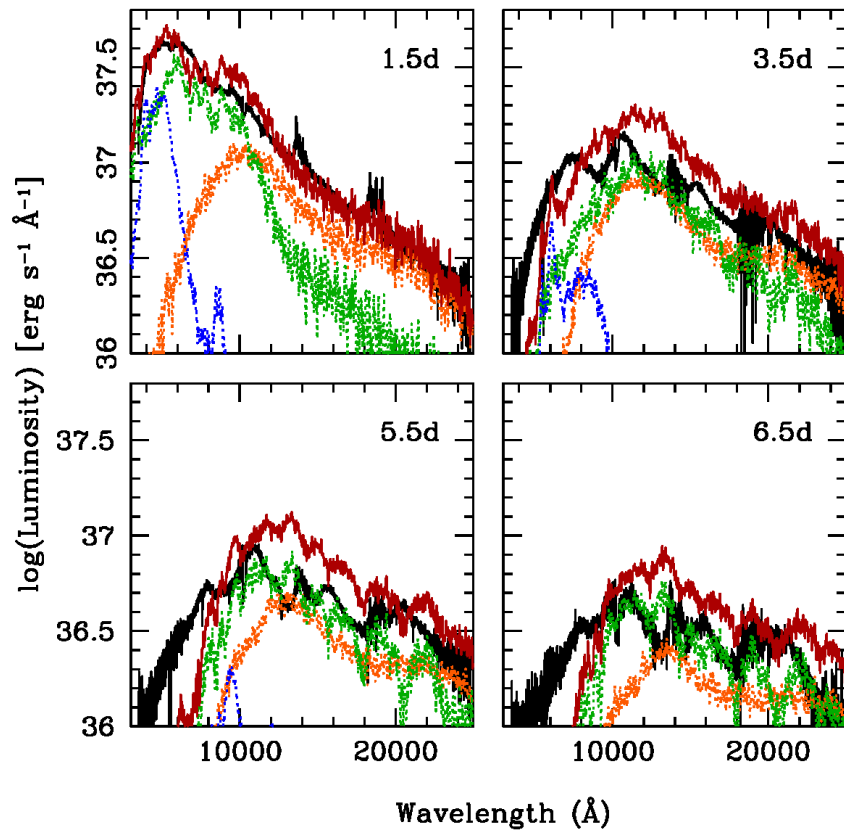
**Figure 5.** *Left Panel:* Angle averaged synthetic light curves of various wind models at optical blue wavelengths (3500 – 5000 Å). The closed circles show r-band observations of the possible kilonova following GRB 080503 (Perley et al. 2009). The triangle symbol denotes an upper limit. As the redshift of 080503 is unknown, we adopt a value  $z = 0.25$  and neglect k-correction effects. *Right Panel:* Model light curves of the same models at infrared wavelengths (1 – 3 μm). The square shows the Hubble Space Telescope observations of the possible kilonova associated with GRB130603B (Tanvir et al. 2013; Berger et al. 2013).



Observed light curve GW 170817 vs a two component model for the r-process (Cowperthwaite et al ApJ, 2017)

**Table 1**  
Kilonova Model Fits

Model	$M_{ej}^{blue}$ ( $M_{\odot}$ )	$v_{ej}^{blue}$ (c)	$\kappa^{blue}$ ( $cm^2 g^{-1}$ )	$M_{ej}^{purple}$ ( $M_{\odot}$ )	$v_{ej}^{purple}$ (c)	$\kappa^{purple}$ ( $cm^2 g^{-1}$ )	$M_{ej}^{red}$ ( $M_{\odot}$ )	$v_{ej}^{red}$ (c)	$\kappa^{red}$ ( $cm^2 g^{-1}$ )	$f^{Ni}$	WAIC
2-Comp	$0.014^{+0.002}_{-0.001}$	$0.266^{+0.007}_{-0.002}$	(0.5)	...	...	...	$0.036^{+0.001}_{-0.002}$	$0.123^{+0.012}_{-0.014}$	$3.349^{+0.364}_{-0.337}$	...	-102
3-Comp	$0.014^{+0.002}_{-0.001}$	$0.267^{+0.006}_{-0.011}$	(0.5)	$0.034^{+0.002}_{-0.002}$	$0.110^{+0.011}_{-0.010}$	(3.0)	$0.010^{+0.002}_{-0.001}$	$0.160^{+0.030}_{-0.025}$	(10.0)	...	-106



Kilonova model compared to the AT 2017gfo spectra. X-shooter spectra (black line) at the first four epochs and kilonova models: dynamical ejecta ( $Y_e = 0.1 - 0.4$ , orange), wind region with proton fraction  $Y_e = 0.3$  (blue) and  $Y_e = 0.25$  (green). The red curve represents the sum of the three model components.

Pian et al (Nature 2017)